Available online at www.sciencedirect.com
SCIENCE DIRECT®
Coordination Chemistry Reviews 249 (2005) 1620–1640
COORDINATION CHEMISTRY REVIEWS
www.elsevier.com/locate/ccr

Review

DFT investigations of models related to the active site of [NiFe] and [Fe] hydrogenases

Maurizio Bruschi [a], Giuseppe Zampella [b], Piercarlo Fantucci [b], Luca De Gioia [b,*]

[a] *Department of Environmental Science, University of Milano-Bicocca, Piazza della Scienza, 120126 Milan, Italy*
[b] *Department of Biotechnology and Biosciences, University of Milano-Bicocca, Piazza della Scienza, 220126 Milan, Italy*

Received 9 July 2004; accepted 3 December 2004
Available online 19 March 2005

Abstract

Density functional theory (DFT) has been recently used to explore the chemistry of models of the active site of [NiFe] and [Fe] hydrogenases, which are enzymes that catalyse the reversible oxidation of H_2.

Results from recent theoretical investigations aimed at characterizing relevant intermediate species in the catalytic cycle of hydrogenases, clarifying the structural and electronic properties of the bimetallic cofactors, as well as the key factors responsible for H_2 activation, are reviewed. The role of theoretical contributions in the investigation of synthetic models related to the enzymatic metal cofactors is also discussed, showing how 'in silico' coordination chemistry can nicely complement experimental studies in the characterization of relevant species.

Keywords: Transition metal ions; Bioinorganic chemistry; Nickel; Iron; Hydrogen activation

Contents

* Corresponding author. Tel.: +39 02 64483463; fax: +39 02 64483478.
E-mail address: luca.degioia@unimib.it (L. De Gioia).

0010-8545/$ – see front matter © 2004 Elsevier B.V. All rights reserved.
doi:10.1016/j.ccr.2004.12.007

1. Introduction

1.1. Hydrogenases

Hydrogenases are enzymes that catalyse the reversible cleavage of dihydrogen according to the reaction:

$$H_2 \leftrightarrows 2H^+ + 2e^-$$

These enzymes contain transition metal ions and, according to the metal ions found in the active site, have been classified as [NiFe] or [Fe] hydrogenases [1]. Remarkably, also enzymes previously classified as 'metal-free' hydrogenases have been recently shown to contain an iron-containing cofactor of functional importance [2].

The three-dimensional structures of [NiFe] and [Fe] hydrogenases have been determined by X-ray diffraction [3–9], revealing the structural organization of these enzymes and disclosing the unusual features of the metal cofactors involved in H_2 activation.

In the active site of [NiFe] hydrogenases, a nickel ion is bound to the protein by four cysteine residues, two of which are coordinated also to an iron ion. The coordination environment of iron is completed by two CN^- and one CO ligands, which have been characterized by IR spectroscopy [10]. In the 'as isolated' catalytically inactive form of the enzyme an additional oxygen-containing ligand bridges the two metal ions (Fig. 1a) [3].

Kinetic and spectroscopic studies led to the characterization of several redox states. Four paramagnetic forms of [NiFe] hydrogenases (usually referred to as Ni-A, Ni-B, Ni-C, Ni-L) have been identified. The Ni-A form is very slowly activated in the presence of H_2, whereas Ni-B is quickly activated under the same conditions [11]. The Ni-C form, which is catalytically active, is two electrons more reduced than Ni-B [12]. Upon illumination of the Ni-C form, a new species (Ni-L), which is stable at temperature below 100 K, is generated. EPR silent forms, referred to as Ni-SU, Ni-SI and Ni-R, have also been identified and the number of protons involved in their interconversion have been determined (Scheme 1) [1,13,14].

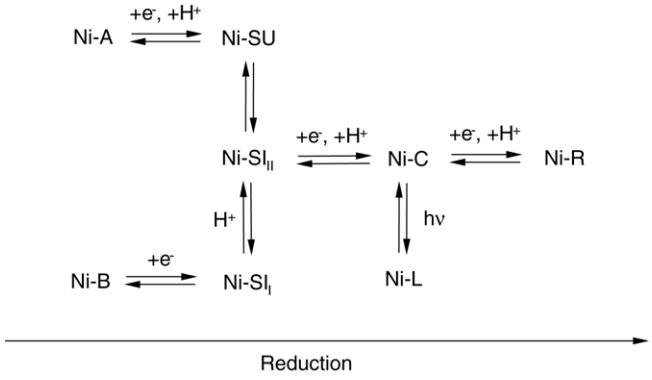

Scheme 1. Redox states of [NiFe] hydrogenases characterized by spectroscopic techniques.

The active site of [Fe] hydrogenases contains an unusual $[Fe_6S_6]$ cluster, referred to as the H-cluster, which is composed by a regular $[Fe_4S_4]$ cluster bridged by a cysteine residue to a binuclear subcluster ($[2Fe]_H$) where the cleavage of dihydrogen is thought to take place (Fig. 1b)

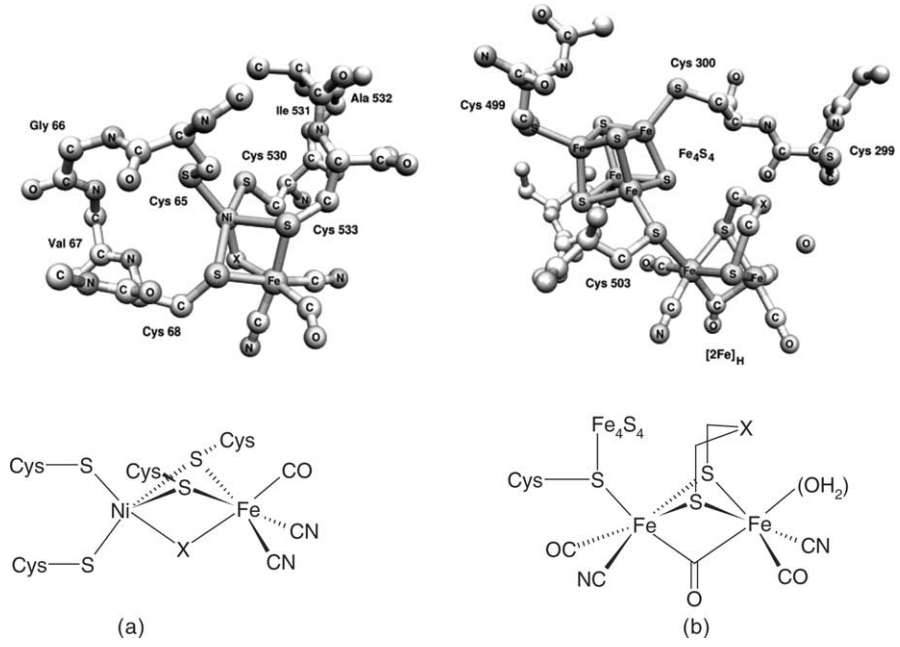

Fig. 1. Structure of the bimetallic clusters found in the active site of [NiFe] (a) and [Fe] hydrogenases (b). X has been proposed to correspond to O^{2-} or OH^- and CH_2 or NH, in parts (a) and (b), respectively. The aminoacids surrounding the [NiFe] and [Fe] hydrogenase active sites have been numbered according to the sequence from *Desulfovibrio gigas* and *Clostridium pasteurianum*, respectively.

[9]. The two iron atoms of $[2Fe]_H$, referred to as proximal (Fe_p) and distal (Fe_d) with respect to the bridging cysteine residue, are coordinated by CO and CN^- ligands and by a chelating S–X_3–S moiety, where X_3 is composed of covalently bound light atoms. The nature of the X atoms is still uncertain and both di(thiomethyl)amine (DTMA) and 1,3-propanedithiolate (PDT) have been proposed as plausible chelating groups [9]. Spectroscopic investigations of [Fe] hydrogenases are consistent with a +2 oxidation state for the $[Fe_4S_4]$ cluster, both in the oxidized and reduced forms of the H-cluster [15]. Three redox states for the $[2Fe]_H$ subcluster have been characterized [16]. In the fully oxidized and fully reduced forms, the bimetallic cluster is EPR silent, whereas the partially oxidized form is paramagnetic. In the oxidized inactive form of the enzyme, a CO group bridges the iron atoms of the $[2Fe]_H$ cluster and a coordination site on Fe_d is occupied by an oxygen containing species (OH^- or H_2O), which is replaced by a CO group in the CO-inhibited, oxidized form [17]. X-ray and FT-IR data indicate that the μ-CO group switches to semibridging or terminal position going from the oxidized to the reduced form of the enzyme [18].

1.2. Synthetic models of hydrogenase active sites

The disclosure of the structural features of [NiFe] and [Fe] hydrogenases has stimulated efforts toward the synthesis of organometallic compounds featuring the essential attributes of the bimetallic clusters found in the enzymes active site [19,20].

The first complexes resembling to some extent the enzymatic metal cofactor of [NiFe] hydrogenases were synthesised in the laboratories of Darensbourg and coworker [20], and Pohl and coworkers [21]. NiFe complexes showing some structural features of the enzyme active site were also reported by Evans and coworkers [22], and by Schroder and coworkers [23]. Recently, the first dinuclear NiFe complex in which the nickel ion is coordinated only by thiolate groups has been reported by Sellman et al. [24].

The observation that the $[2Fe]_H$ cluster in the active site of [Fe] hydrogenase is similar to well known organometallic compounds characterized by the general structure $[Fe_2(\mu\text{-}SR)_2(CO)_6]$ (where R is an organic group) [25], led three research groups to the simultaneous report of the synthesis of the complex $[Fe_2(SCH_2CH_2CH_2S)(CO)_4(CN)_2]^{2-}$ [26]. After the proposal that DTMA could be the chelating ligand and bridging the Fe ions in the $[2Fe]_H$ cluster, Rauchfuss and coworkers reported the synthesis and characterization of $[Fe_2(SCH_2NHCH_2S)(CO)_4(CN)_2]^{2-}$ [27]. A further step forward to obtain synthetic models even more closely related to the $[2Fe]_H$ cluster has been done by Pickett and coworkers, which have shown that the backbone modification of a propane dithiolate ligand can lead to organometallic complexes characterized by the Fe_2S_3 ligation observed in the enzyme [28]. Novel single and double di-iron models for the active site of [Fe] hydrogenases have also been recently reported by Song et al. [29].

2. Quantum chemical investigation of hydrogenases

The reliability of quantum chemical methods to study simple models of metal enzymes is nowadays well grounded [30]. In fact, theoretical results can be very useful for interpretation and rationalization of experimental data. In addition, quantum chemical investigations can discriminate among alternative reaction mechanisms and identify intermediate species too short-lived to be characterized experimentally. Moreover, even when a complete picture of the chemistry is available, theoretical investigations can help to explain why a particular reaction path is favoured with respect to others. Finally, 'in silico' coordination chemistry can allow, in a relatively cheap way, to explore synthetic pathways and chemical properties of coordination compounds not yet experimentally characterized, stimulating and possibly driving synthetic efforts.

In this contribution, recent theoretical results obtained investigating models related to the active site of [NiFe] and [Fe] hydrogenases are reviewed. In this context, the contributions from the laboratories involved in theoretical studies are particularly interesting because many of the above mentioned possibilities offered by quantum chemistry have been critically used to explore the properties of the enzymatic cofactors, as well as of related synthetic systems. It should be noted that theoretical investigations of [NiFe] hydrogenase models have been already reviewed [31], covering papers published from 1998, when the first study of the catalytic properties of the heteronuclear bimetallic cluster was reported [32], to 2002. Therefore, for investigations related to [NiFe] hydrogenases, we will focus mainly on results reported in the last two years, briefly discussing older contributions only to present a general overview.

2.1. Theoretical methods and model descriptions

Theoretical investigations of models related to the active site of [NiFe] and [Fe] hydrogenases have been carried out mainly within the framework of Density Functional Theory (DFT) [33], even though the investigation of models of the [NiFe] hydrogenase active site using semiempirical quantum chemical methods has recently been reported [34].

A thorough coverage of DFT implementations, strengths and limitations has been recently reported [35]. DFT is based on the fundamental theorem [36] which proves the existence of a functional of the electron density that contains all the energy contributions, including the so called correlation contributions, which are related to the behaviour and mutual interaction of groups of electrons. This latter aspect is just the fundamental difference between DFT and the conventional Hartree–Fock (HF) theory. As well known, the HF method neglects correlation effects as each single electron is supposed

to move in a mean field provided by all other N-1 electrons. In the past, several methods have been proposed and used to go beyond the HF limit, by introducing correlation effects via post-HF corrections, all of them inspired to different extent by the configuration interaction (CI) method [37]. While HF builds the (single configuration) wave function by means of one-electron functions (the molecular orbitals, MO), the CI method obtains the molecular wave function as linear combination (energy optimised) of many-electron functions (the HF-like wave functions). The HF method, among the so called "ab initio" approaches, provides the cheapest way to obtain a molecular wave function, whereas the CI correction (in all its possible variants) applied in post-HF methods is generally extremely time consuming. On the contrary, the computational time required by DFT calculations is only slightly larger than for HF, offering at the same time several advantages:

(i) The DFT method keeps a one-electron structure similar to the HF one thus offering a much easier interpretation of the results while incorporating the correlation effects.
(ii) The DFT description of open-shell systems is much more balanced than the HF description, which is known to enhance the importance of high-spin contributions.
(iii) When open-shell systems are treated at the "unrestricted" level (different MOs for different spin), the DFT solution is generally contaminated by high multiplicity contributions to a much lesser extent than the HF one. Thus, DFT wave functions are usually quite close to a pure spin representation [38].
(iv) DFT methods are found to give excellent results for molecular systems characterized by near-degenerate states, which are generally not adequately described by ab initio mono-determinantal perturbational theories (for example, MP2).

However, DFT methods are not free from limitations: the accuracy of DFT results cannot be increased systematically, as it occurs with the fully ab initio approaches making use of strictly variational methods and wavefunction expansions. In addition, the limitations inherent to the adopted exchange-correlation functional cannot be a priori removed, since the exact form of the functional remains unknown. As a consequence, the reliability of a given functional can be only established in a heuristic way, by comparison of the DFT results with the experiments or, when possibile, with extremely accurate results obtained from highly correlated ab initio methods. In this context, coordination compounds represent one of the most difficult cases, because very accurate ab initio results are, in general, not available.

In spite of the above limitations, DFT has become a general tool to investigate models of metal-containing proteins. In fact, the recently developed functionals based on the generalised gradient approximation (GGA) and the so-called hybrid methods, in which a percentage of Hartree–Fock exchange energy is added to the exchange-correlation energy, give accuracies similar or higher than ab initio MP2 methods, but with the advantage of a computational cost that is comparable to Hartree–Fock calculations. In addition, recent techniques developed to calculate the Coulomb energy, such as the Resolution of Identity (RI) approximation [39], have further improved the computational efficiency.

The hybrid three parameter B3LYP and the pure BP86 functionals have been widely used in computational studies of models of the active site of [NiFe] and [Fe] hydrogenases. The hybrid B3LYP functional [40], which was originally calibrated on the G2 database of organic molecules, is now commonly used to study also metal-containing molecular systems, due to the increasing available computational data which indicate that B3LYP, coupled with an appropriate basis set, predicts accurately properties as bond dissociation energies and molecular geometries ([30] and references therein). Analogous considerations hold true for BP86 [41], which was shown to be one of the most accurate pure functionals to study transition metal compounds [42]. In fact, both B3LYP and BP86 usually reproduce experimental geometries within a few hundredths of an Å, and also reaction energies can be generally predicted with a reasonable accuracy, even though in some cases computed values can be quite dramatically affected by the adopted functional and basis set [35,43]. Other relevant experimental observables such as spin densities, EPR hyperfine coupling constants, *g*-tensors and vibrational frequencies can be presently computed with a sufficiently high accuracy within the DFT framework to allow the comparison with the corresponding experimental data [30,35]. FT-IR spectra are extremely useful for the characterization of intermediate species and redox states of [NiFe] and [Fe] hydrogenases ([1] and references therein), as well as of related model complexes ([19] and references therein), due to the peculiar vibrational frequencies of the CN and CO groups. In particular, the calculation of vibrational frequencies and their comparison with experimental data has been used extensively to validate theoretical protocols and to predict the structural features of intermediate species relevant to [NiFe] and [Fe] hydrogenase chemistry (see below). Note that the computation of vibrational frequencies is also necessary to check the curvature of the potential energy surface around the stationary point, in order to distinguish a true minimum (all vibrational frequencies are positive) or a transition state (one imaginary vibrational frequency), and to calculate the zero point energy correction to the electronic energies in order to obtain accurate thermodynamic data. As for the accuracy of computed vibrational frequencies, it is well know that, due to the harmonic approximation adopted in the calculation of force constants, the vibrational frequencies computed with ab initio methods are systematically higher than the experimental ones [43]. Therefore, empirical correction factors are often used to improve the agreement with the experiment. For example, at the HF/6-31G* level of theory, a correction factor of 0.8953 is commonly used to scale the calculated frequencies [44]. Vibrational frequencies computed using DFT methods have generally a higher accuracy than those obtained at HF

level and similar to that obtained with correlated ab initio methods. In the specific case of CO and CN groups in [NiFe] and [Fe] hydrogenase models, wave numbers obtained from BP86 calculations with harmonic approximation compare extremely well with experimental data [45,46], even if the excellent agreement is partially due to an error cancellation effect [47].

Calculations of *g* and hyperfine tensors, taking into account relativistic effects and spin–orbit couplings, have been recently carried out in the framework of DFT [48]. In particular, DFT calculations have been carried out within the 'Zero-Order Regular Approximation' (ZORA) [49], using both local VWN [50] and gradient corrected (BP86) functionals. Even though further improvements in the accuracy of computed magnetic properties is needed and might be expected to arise when simultaneously considering spin-polarization and spin–orbit coupling [51], theoretical results generally agree reasonably well with experimental data [52–54].

A very important methodological issue related to the theoretical investigation of [NiFe] and [Fe] hydrogenase concerns the design of the computational models, which are always the result of a compromise between a realistic representation of the system and the necessity to treat relatively small models in order to reduce computation time. In fact, most investigations have been carried out using simple models, where the side chains of the cysteine residues coordinated to the metal ions have been modelled by H or CH_3 groups. The choice of both CH_3S^-, and CH_3SH as model of the cysteine residue bridging the $[Fe_4S_4]$ and the $[2Fe]_H$ clusters in [Fe] hydrogenases was driven by the necessity to keep into account in a simple way possible changes in the oxidation state of the $[Fe_4S_4]$ cluster.

Calculations carried out on model systems including all aminoacids in the first and second coordination sphere of the metal clusters have been reported [55]. Indeed, the investigation of small and large systems can give access to complementary information. Small models are computationally less expensive and consequently their investigation is generally carried out using sophisticated approaches and sampling extensively the structural and electronic properties. On the other hand, larger models are particularly suited to investigate properties that might be influenced by the protein environment.

2.2. [NiFe] hydrogenases

2.2.1. The structure of the bimetallic cluster in different redox states

Different research groups have used DFT to predict the structure of the active site in the spectroscopically characterized states of [NiFe] hydrogenases (Scheme 1) [31]. Paramagnetic Ni(III) redox states (Ni-A, Ni-B, Ni-C, Ni-L) have been the most thoroughly investigated. Several studies converged on the proposal that the Ni-A redox state should be characterized by the presence of O^{2-} or OH^- bridging the metal centres [31]. Either structures characterized by a μ-OH group or by the absence of small ligands bridging the two metal ions were initially proposed for Ni-B [31]. However, the electronic properties of Ni-B models characterized by a vacant coordination position between the two metal ions are not fully consistent with spectroscopic data [56].

Lubitz and coworkers have recently compared experimental and computed magnetic properties for several Ni(III) species to discern among different possible structures of the bimetallic cluster [52]. Computation of *g* tensors and hyperfine tensors led to the conclusion that a μ-OH group is present in the Ni-B redox state. Stadler et al. reached similar conclusions [53], proposing that a μ-hydroxo group is present in both Ni-A and Ni-B. According to the latter study, the differences in the electronic structures of Ni-A and Ni-B can be explained by a different protonation state of one terminal cysteine residue.

It is believed that the bimetallic cluster undergoes a Ni(III)/Ni(II) redox shuttle during catalysis (Scheme 1) and that the paramagnetic Ni-C form is an intermediate species in the catalytic cycle. DFT results led to the conclusion that Ni-C corresponds to a Ni(III) species in which a H atom bridges the metal centres [56]. Moreover, the presence of a μ-H in Ni-C is compatible with experimental EPR and IR data [31]. In particular, Lubitz and coworkers compared the experimental *g* tensor magnitudes and orientations for the Ni-C and Ni-L forms with those predicted by DFT calculations for several models of the active site [54]. Good agreement between experiment and theory was obtained for Ni-C and Ni-L forms corresponding to Ni(III) species where a hydride bridges the two metal atoms, and to Ni(I) species with a vacant bridge position, respectively. In addition, the unpaired electron of Ni-C was assigned to the $3d_{z^2}$ orbital, whereas for Ni-L a substantial fraction of the unpaired electron was found in the $3d_{x^2-y^2}$ orbital.

Unfortunately, many experimental and theoretical approaches used to characterize the Ni-A, Ni-B and Ni-C redox states cannot be exploited for the characterization of EPR-silent species, and consequently structural and electronic properties of Ni(II) intermediate species are more elusive and still controversial. In fact, several studies converge to the proposal that in the Ni-SI redox-state the Ni(II) ion is four-coordinated [31], even though Stein and Lubitz recently proposed that, in the Ni-SI form, H_2 and H_2O are coordinated to Ni and Fe, respectively [51] (Fig. 2). Either structures characterized by a μ-H atom or structures where H_2 is coordinated to the iron centre have been proposed for the Ni-R form. In particular, De Gioia et al. showed that a μ-H Ni(II)Fe(II) species has the proper stereoelectronic characteristics to correspond to the Ni-R redox state [56], following previous proposals formulated on the ground of experimental studies [57]. Stein and Lubitz reached similar conclusions, even though according to their proposal, two H atoms are simultaneously coordinated to the Ni ion in the Ni-R form [51]. Hall and coworkers concluded, on the basis of relative stability data, that H_2 is not yet cleaved and is bound in a η^2

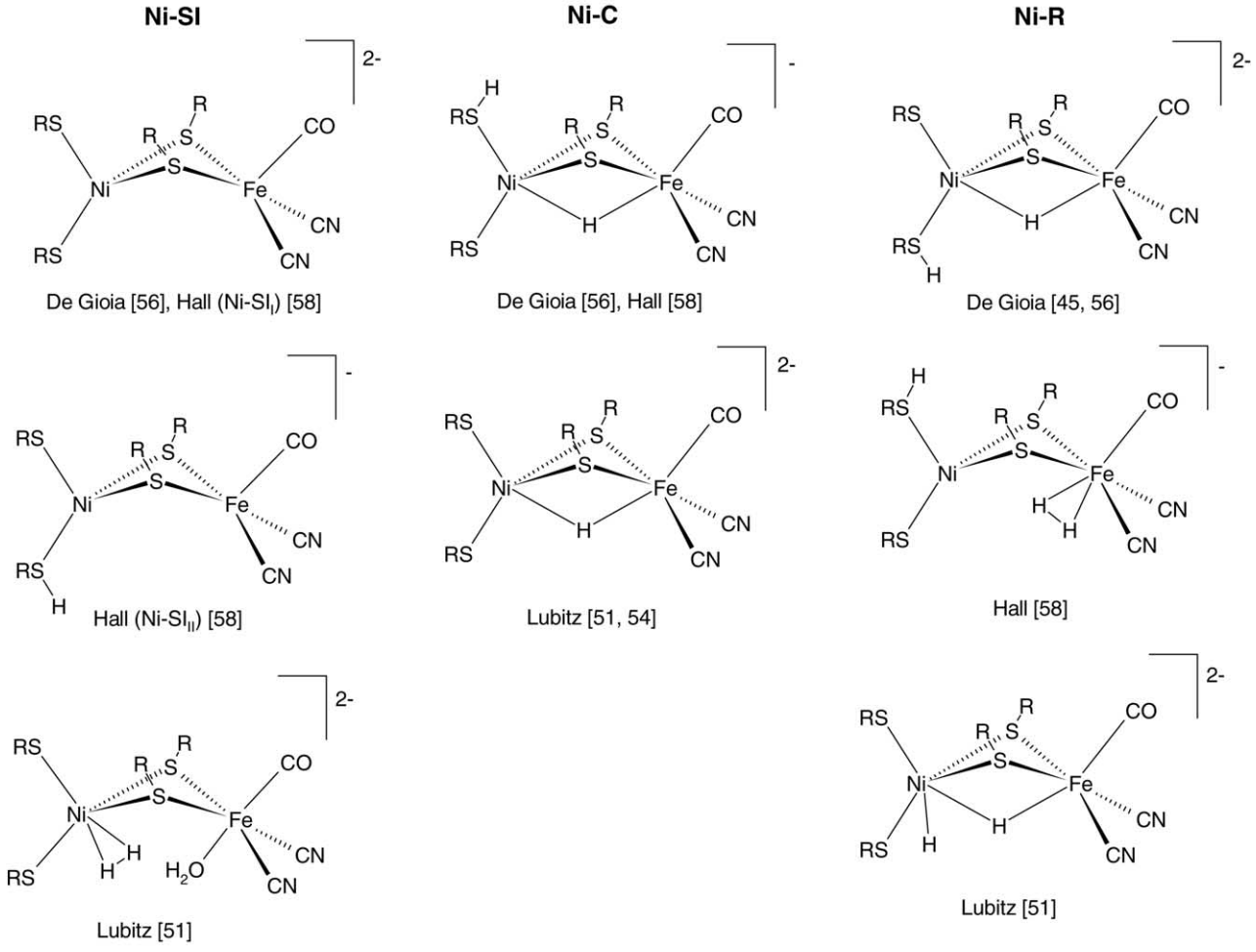

Fig. 2. Structures of redox states relevant for the catalytic cycle of [NiFe] hydrogenases, as proposed by different research groups on the ground of DFT investigations.

fashion to the Fe centre in the Ni-R redox state of the enzyme. However, the possibility that Ni-R could correspond to a μ-H species was not excluded [58].

Another controversial issue is related to the ground state of the Ni(II) ion in the Ni-SI and Ni-R forms. Until recently, spectroscopic data have been considered to be compatible with a diamagnetic ($S = 0$) ground state for the Ni(II) ion [57,59], and therefore theoretical models of Ni-SI and Ni-R were computed assuming a singlet state. Indeed, it was noted that, for Ni-SI models, this assumption leads to structures characterized by a slightly distorted square planar coordination environment of the nickel ion [31,56,60], which is not compatible with the X-ray structures of the 'as isolated' form of the enzyme [3], and therefore would imply a large structural rearrangement of the cysteine ligands in the active site. Remarkably, recently reported nickel L-edge soft X-ray data have suggested the possible formation of high-spin ($S = 1$) Ni(II) species in the catalytic cycle of [NiFe] hydrogenases [61], and this observation has stimulated further theoretical investigations aimed at shedding light on this crucial aspect. Hall and coworkers [62] have used B3LYP to show that high spin (triplet) models of the Ni-SI and Ni-R redox forms are characterized by a distorted tetrahedral Ni coordination environment that fits well with the structure of the bimetallic cluster observed in the X-ray structure of the reduced forms of the enzyme [5,7]. It was also noted that, even though high spin forms are computed to be only slightly more stable than corresponding low spin species, the energy gap in favour of high spin species could be even larger if the protein resists the rearrangement of the Ni coordination geometry from tetrahedral to square planar.

As discussed in Section 2.1, most of the computational studies of [NiFe] hydrogenase models have been carried out using the B3LYP functional [40], on the ground of its high accuracy in reproducing structures, electronic properties and relative energies of organic and inorganic compounds [63,64]. However, it has been recently shown that B3LYP predicts the wrong multiplicity of the ground state for some transition metal complexes [65,66]. Nonhybrid functionals can be affected by similar problems [67], and these observations have stimulated efforts to test, calibrate and tune different functionals for their use in the investigations of

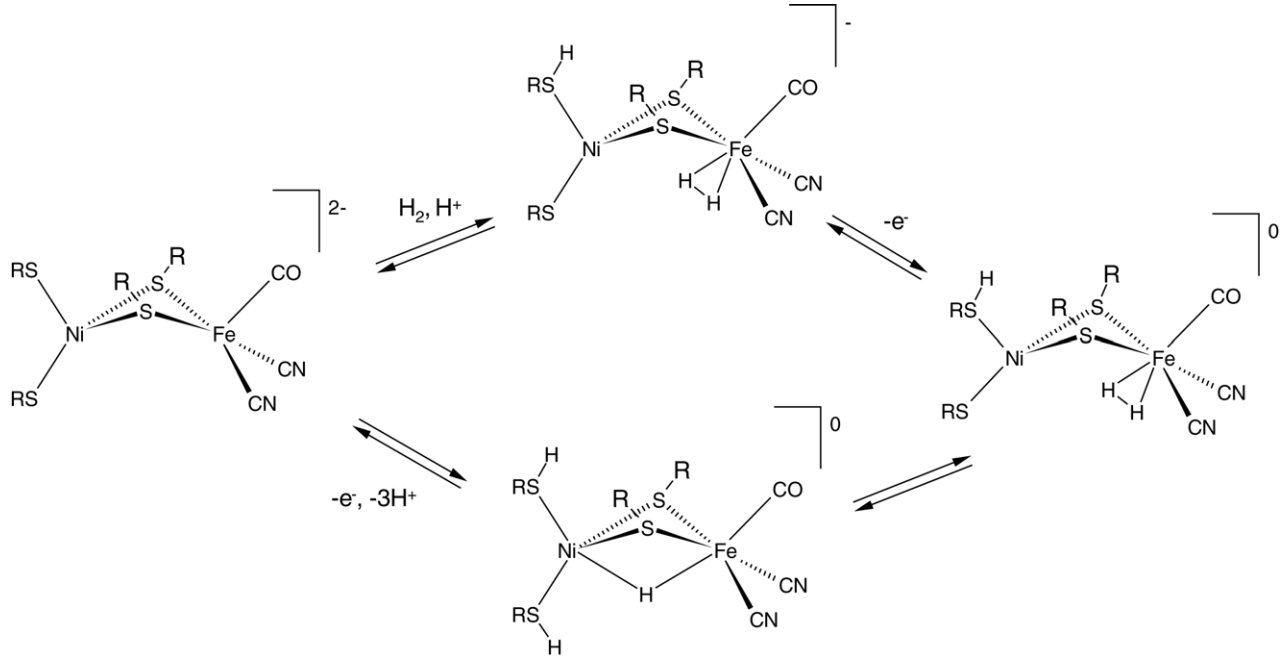

Fig. 3. Catalytic cycle of [NiFe] hydrogenases proposed by Hall and coworkers [58,71] on the ground of DFT investigations.

coordination compounds [68,69]. Prompted by these studies and with the main goal to investigate the effects of pure and hybrid functionals on computed properties of Ni(II) ions in thiolate-rich environments, Bruschi et al. have very recently studied the structural and electronic properties of well-characterized high- and low-spin [Ni(II)S_4] complexes, as well as high- and low-spin Ni(II)Fe(II) models of the [NiFe] hydrogenase active site [45]. The comparison of results obtained with BP86 [41], B3LYP [40] and B3LYP* [69,70] led to the conclusion that BP86 is the most suited functional to describe the structural features of [Ni(II)S_4] complexes, whereas the prediction of the ground state, as well as the relative stability of high and low spin states, is more problematic and may be dependent on the adopted functional. Results obtained investigating Ni(II)Fe(II) models confirmed that the structure of the bimetallic cluster, as observed in the X-ray structure of the reduced form of the enzyme [5,7], is compatible with the presence of a hydride bridging the

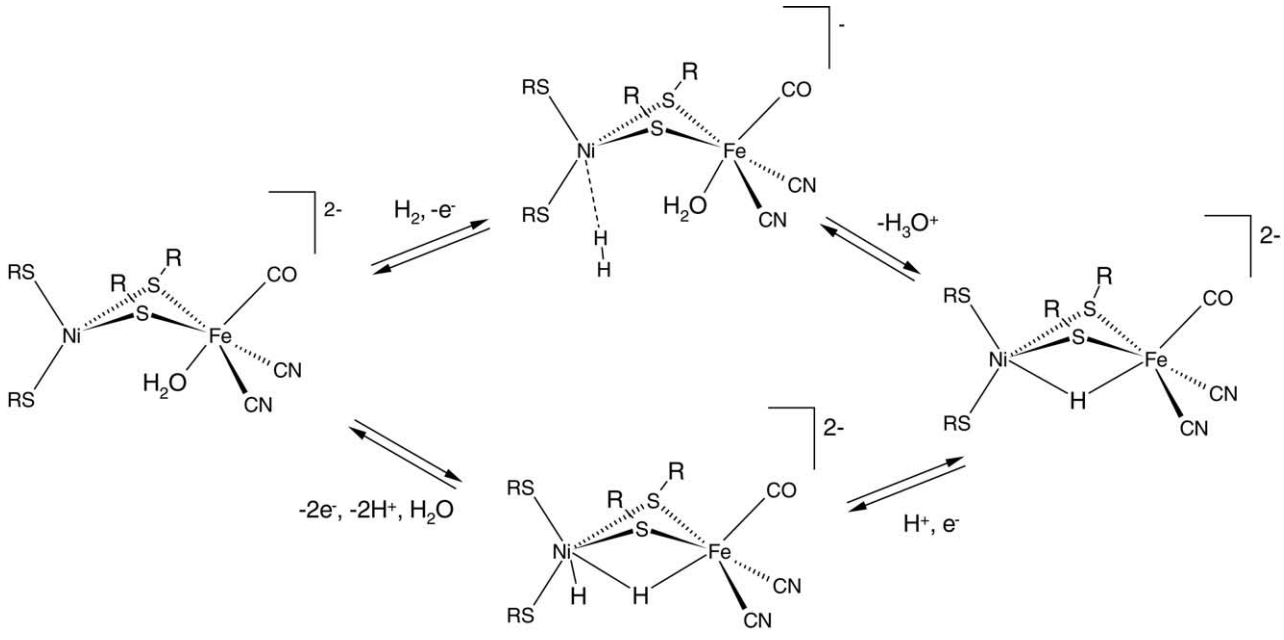

Fig. 4. Catalytic cycle of [NiFe] hydrogenases proposed by Stein and Lubitz [51] on the ground of DFT investigations.

two metal centres. It was also concluded that both Ni-SI and Ni-R are potential spin-crossover species. However, while the high–low spin interconversion in Ni-SI is accompanied by a large reorganization of the Ni coordination environment (from tetrahedral to square planar), the corresponding interconversion in the μ-H Ni-R form is accompanied by negligible structural rearrangements, indicating that it can easily take place within the enzyme active site [45].

2.2.2. The catalytic mechanism

Structures, electronic properties and relative energies computed for several models of the bimetallic cluster found in the active site of [NiFe] hydrogenases led to the proposal of plausible catalytic cycles for H_2 activation and cleavage. Results from different groups converge on many details, such as the proposal that dihydrogen activation should eventually imply proton transfer to one of the cysteine residues coordinated to the nickel ion. However, the site of H_2 binding and the redox state of the bimetallic cluster in the H_2 activation step are still controversial.

The first DFT investigation of the catalytic mechanism of [NiFe] hydrogenases was reported by Siegbahn and coworkers, which proposed that H_2 first binds to Fe and in the key step hydride transfer to iron and proton transfer to the adjacent cysteinethiolate ligand are accompanied by decoordination from Ni of the protonated cysteinethiol [32].

According to Hall and coworkers [58] (Fig. 3), H_2 binds to the bimetallic cluster leading to a Ni(II)Fe(II) Ni-R form where H_2 is coordinated to the iron centre. Binding of H_2 should also trigger one-electron oxidation of the cluster. In fact, on the basis of computed relative energies, it was concluded that heterolytic cleavage of H_2 is more exothermic on Ni(III) species than on the corresponding Ni(II) form. To obtain a more detailed picture of the H_2 cleavage step, Niu and Hall have investigated also transition state structures and energy barriers along the nucleophilic addition pathway involving a Ni(III) species, using both a neutral ($[(CO)(CN)_2Fe(\mu\text{-}SH)_2Ni(SH)(SH_2)]$) and an anionic ($[(CO)(CN)_2Fe(\mu\text{-}SH)_2Ni(SH)_2]^-$) model of the enzyme cofactor [71]. Remarkably, the computed transition state structures showed a striking resemblance to the structure of the cluster observed in the X-ray structure of the enzyme (Fig. 1a).

Also Stein and Lubitz [51] proposed a mechanism in which H_2 activation takes place on a Ni(III) species. The reaction pathway implies the binding of dihydrogen to the Ni ion and the participation of a water molecule as the basic residue involved in the heterolytic cleavage (Fig. 4). In particular, in Ni-SI the Ni(II) ion is four coordinated and a water molecule occupies a coordination site of the octahedral Fe(II) ion. Binding of H_2, which takes place to the Ni ion, is proposed to be concomitant with one-electron oxidation of the bimetallic cluster. Then, following H_2 heterolytic cleavage, a transient μ-H species corresponding to Ni-C is formed. One-electron reduction and proton binding leads to a Ni-R species where one H atom is bridged between the metal centres and the other is coordinated to the Ni ion. The catalytic cycle is closed when two electrons and two protons are released to form again the Ni-SI species.

Starting from a previous proposal based on spectroscopic data [57], De Gioia et al. characterized structures and electronic properties of possible intermediate species formed in a catalytic cycle that implies dihydrogen activation on a Ni(II)Fe(II) species (Fig. 5) [56]. According to this proposal, heterolytic cleavage of dihydrogen takes place by a nucleophilic addition pathway involving one of the cysteine

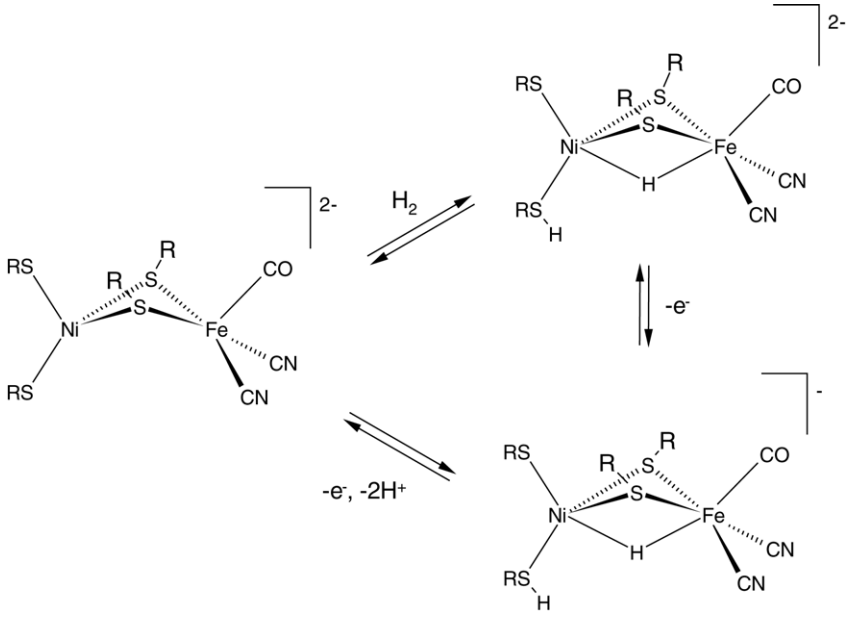

Fig. 5. Catalytic cycle of [NiFe] hydrogenases proposed by De Gioia et al. [56] on the ground of DFT investigations.

ligands coordinated to the Ni centre. This step leads to a μ-H Ni(II)Fe(II) species that was proposed to correspond to Ni-R. Monoelectron oxidation of Ni-R leads to the paramagnetic Ni-C redox state, in which a hydride is still bridged between the two metal ions. Finally, the catalytic cycle is closed by release of two protons and one electron. It has been recently shown [45] that also the relative stability of the Ni-SI and Ni-R structures initially proposed by Dole et al. [57] are fully compatible with their formation in the catalytic cycle of the enzyme. Moreover, the structural arrangement of the cysteine ligands in high-spin Ni-SI and both in high and low spin Ni-R models closely resembles that observed in the enzyme, and it is therefore compatible with a catalytic cycle that does not imply major structural reorganization of the protein environment.

2.3. [Fe]-hydrogenases

2.3.1. The redox states of the bimetallic cluster

Different redox states of the $[2Fe]_H$ cluster have been characterized spectroscopically. The fully oxidized and fully reduced forms of the enzyme are EPR silent and have been proposed to correspond, on the basis of similarities between the FT-IR spectra of the enzyme and of model compounds, to Fe(II)Fe(II) and Fe(I)Fe(I) species, respectively [19,72]. The partially oxidized form is paramagnetic and should correspond to the Fe(I)Fe(II) redox states, even though Mossbauer data are also compatible with a Fe(III)Fe(II) redox state [15].

The first DFT study aimed at investigating coordination compounds related to the $[2Fe]_H$ cluster was reported by Ian

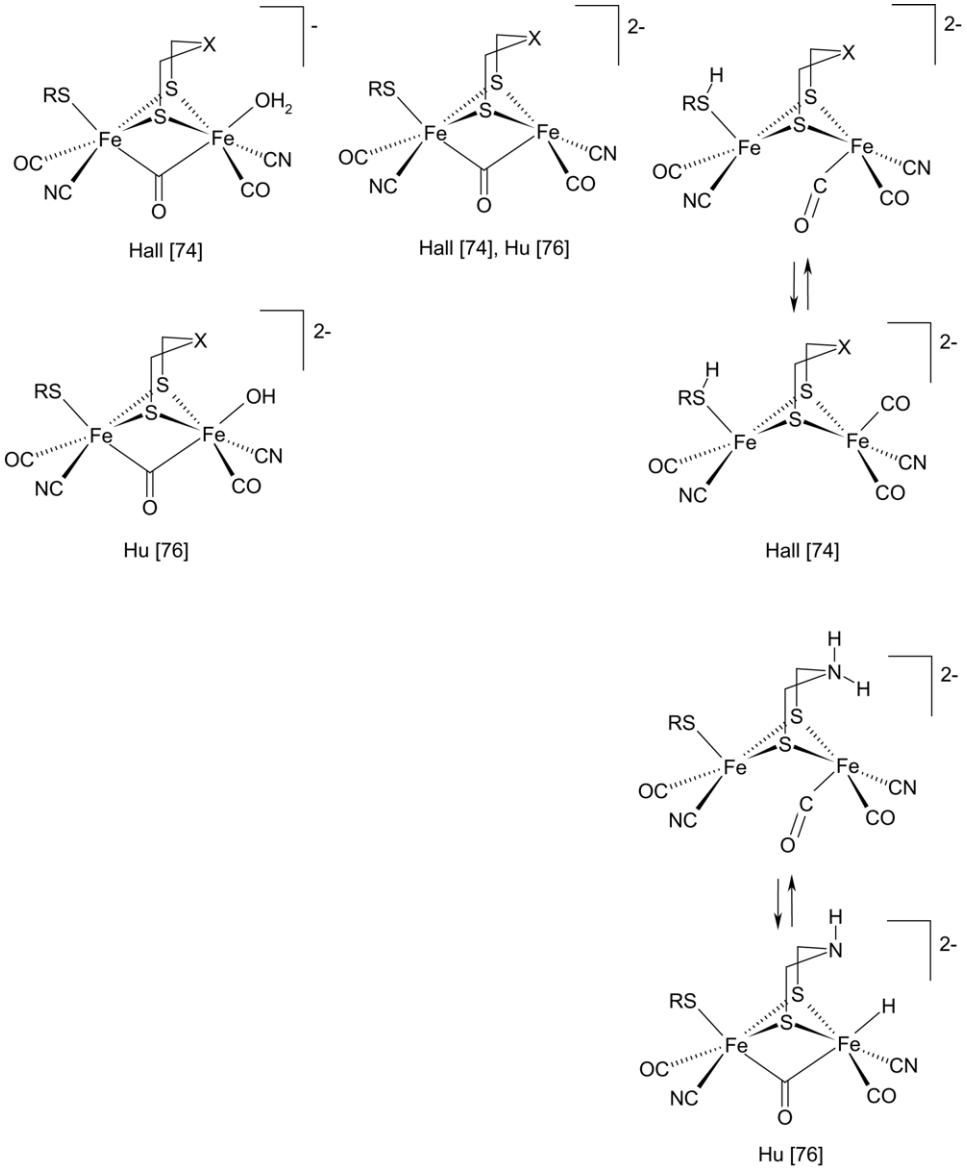

Fig. 6. Structures of the oxidized, partially and fully reduced forms of the $[2Fe]_H$ cluster, as proposed by different research groups on the ground of DFT investigations.

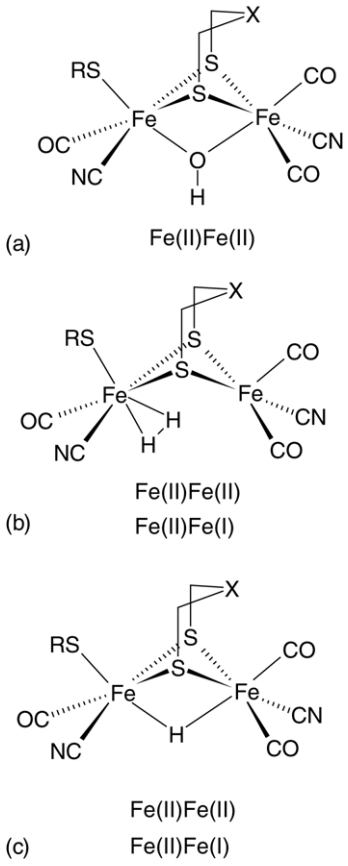

Fig. 7. Other isomers of models of the $[2Fe]_H$ cluster characterized by DFT investigations [77,78].

Dance in 1999 [73]. However, DFT calculations aimed at shedding light on the structural features of the different redox forms were first reported by Cao and Hall [74], which computed structures and vibrational frequencies for the di-iron cluster [(L)(CO)(CN)Fe(μ-PDT)(μ-CO)Fe(CO)(CN)(L′)] (PDT = 1,3-propanedithiolate; L = H_2O, CO, H_2, H^-; L′ = CH_3S^-, CH_3SH). In particular, the excellent correlation between calculated and measured CO and CN^- frequencies found for the synthetic complexes $[Fe_2(CO)_6(\mu\text{-PDT})]$ and $[Fe_2(CO)_4(CN)_2(\mu\text{-PDT})]^{2-}$ allowed to sort out plausible redox states and structures for intermediate species formed in the catalytic cycle of the [Fe]-hydrogenase from *D. vulgaris*, by comparison of computed vibrational frequencies with experimental FT-IR spectra [75]. DFT results showed that the formation of Fe(II)Fe(III) and Fe(III)Fe(III) species is not compatible with FT-IR data. The fully oxidized, EPR silent form, was predicted to correspond to a Fe(II)Fe(II) species, in which a coordination site on the distal Fe centre (Fe_d) is vacant and can bind a water molecule or H_2 (Fig. 6). The partially oxidized form was predicted to correspond to a Fe(I)Fe(II) species characterized by a vacant coordination site on Fe_d and by a CO group bridging the two metal centres. Spin population analysis indicated that the unpaired electron is mainly localized on Fe_d, in agreement with experimental evidences [15]. Finally, it was concluded that both Fe(I)Fe(I) species characterized by one bridging and by all terminal CO groups are compatible with the fully reduced state of the enzyme (Fig. 6).

The structural features of the different redox states were further investigated by Liu and Hu [76], that used a model similar to that used by Cao and Hall [74], except for the PDT chelating ligand that was replaced by DTMA. Comparison between experimental and computed CO stretching frequencies led to the conclusion that the fully oxidized state of the $[2Fe]_H$ cluster is a Fe(II)Fe(II) species in which an OH^- group is terminally coordinated to Fe_d (Fig. 6). The paramagnetic form of the cluster was predicted to correspond to an Fe(I)Fe(II) species, in full agreement with Cao and Hall [74], whereas it was concluded that the fully reduced state is a mixture of two forms, where the major component is a protonated Fe(I)Fe(I) species and the other is an Fe(II)Fe(II) hydride species. It was also concluded that the different redox states differ only for the occupation of a bonding orbital between μ-CO and Fe_d, which is fully occupied only in the Fe(I)Fe(I) form.

Bruschi et al. used DFT to investigate the Fe(II)Fe(II) model $[(\mu\text{-PDT})Fe_2(CO)_3(CN)_2(CH_3S)]^-$ and its H_2O and H_2 adducts, showing that structures characterized by a water molecule or a OH^- group bridged between the two iron centres (Fig. 7a) are more stable than isomers in which a CO bridges the metal centres and the oxygen containing ligand is terminally coordinated to Fe_d [77]. Therefore, it was concluded that if the oxidized form of the enzyme corresponds to a Fe(II)Fe(II) redox state, the μ-OH and μ-H_2O isomers must be destabilized or kinetically

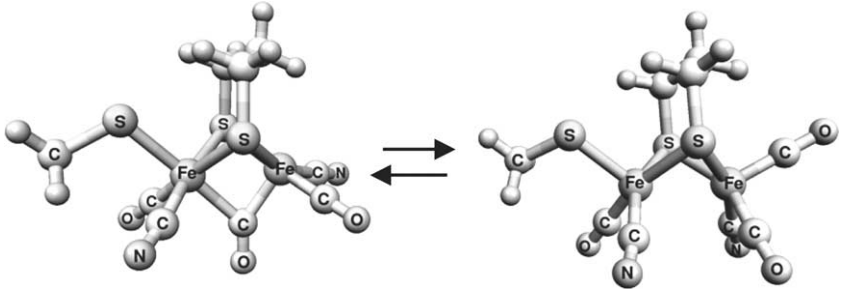

Fig. 8. DFT-optimized structures of isomers of the Fe(I)Fe(II) model complex $[(\mu\text{-PDT})Fe_2(CO)_3(CN)_2(CH_3S)]^{2-}$ [78].

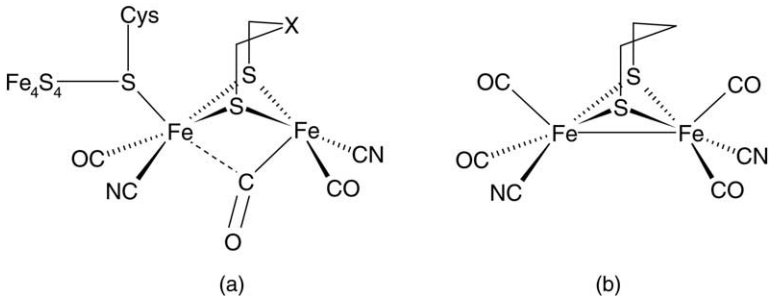

Fig. 9. Comparison between the structures of the fully reduced $[2Fe]_H$ subcluster (a) and a related synthetic Fe(I)Fe(I) model complex (b).

inaccessible within the protein. The DFT characterization of models characterized by a DTMA chelating ligand [78] led to the conclusion that in the Fe(II)Fe(II) model $[(\mu\text{-DTMA})Fe_2(CO)_3(CN)_2(CH_3S)]^-$ the nitrogen atom of DTMA can compete with a water molecule for coordination to the Fe_d ion. Moreover, it was shown that Fe(II)Fe(I) complexes characterized either by the presence or absence of a μ-CO ligand are both stable isomers, and their relative stability is very similar (Fig. 8). In addition, the analysis of computed partial atomic charges revealed that Fe_d is more electrophilic than Fe_p in μ-CO Fe(II)Fe(I) isomers, whereas the opposite is true for the CO-unbridged isomers. As a consequence, H_2 binds to Fe_p and not to Fe_d in CO unbridged isomers (Fig. 7b).

2.3.2. The 'unusual' structural features of the $[2Fe]_H$ cluster

One of the most intriguing aspect of [Fe] hydrogenases is related to the structure of the fully reduced $[2Fe]_H$ subunit. In fact, even though cleverly designed organometallic complexes well reproduce the essential structural features of the dinuclear cluster observed in the enzyme, one striking difference is evident comparing Fe(I)Fe(I) synthetic models and the $[2Fe]_H$ cluster. The former are characterized by an Fe–Fe bond and by terminal CO groups, whereas in the reduced form of the enzyme the Fe_dL_3 group is rotated and consequently a CO group coordinated to the distal iron centres approaches the proximal iron ion and a vacant coordination site appears on Fe_d (Fig. 9) [9,18]. These observations and the results obtained from the NMR investigation of CO_{ap}–CO_{ax} site exchange in binuclear synthetic models [79] prompted Darensbourg and coworkers to carry out DFT calculations aimed at investigating factors affecting the activation barrier for the rotation of the $Fe(CO)_3$ group in the series of binuclear complexes $[Fe_2(\mu\text{-SRS})(CO)_6]$, in which R = edt, pdt or *o*-xyldt [80]. According to computational results, and in good agreement with experimental evidences, $Fe(CO)_3$ rotation is a relatively facile process and the presence of bulky chelating ligands further decreases the activation energy. Moreover, it was noted that the structure of the transition states closely resemble the structure of the $[2Fe]_H$ cluster in the fully reduced state of the enzyme.

The observation that the transition state for $Fe(CO)_3$ rotation resembles the structure of the $[2Fe]_H$ cluster observed in the enzyme, led to the suggestion that the dinuclear cluster could be trapped by the enzyme in an 'entatic state' [81]. However, it was also noted that the presence of good electron-donors in trans to the Fe–Fe bond could stabilize structures with a μ-CO group [82]. This issue was investigated by Bruschi et al. [83], which have studied factors affecting the structural and electronic properties of the $[Fe_2(\mu\text{-PDT})(CO)_3(CN)_2L]$ cluster, where the ligand L, which corresponds to the cysteine side chain coordinated to Fe_p in the enzyme, was systematically replaced by groups with different σ-donor and π-acceptor character (CO, $P(CH_3)_3$, CH_3SH, CN^-, CH_3S^- and CH_3O^-). In the Fe(I)Fe(I) series of complexes, a progressive rotation of the $Fe_d(CO)_2(CN)$ group, whose geometry changes from pseudo square-pyramidal to trigonal bipyramidal, was observed going from the softest (CO) to the hardest (CH_3O^-) L ligand. Concomitantly, a CO group coordinated to Fe_d approaches Fe_p, leading to semibridged structures that, when $L = CH_3S^-$, closely resemble the structure of the $[2Fe]_H$ cluster observed in the reduced form of the enzyme [9] (Fig. 10). Therefore, it was concluded that the substitution in the parent complex $[Fe_2(\mu\text{-PDT})(CO)_6]$ of CO ligands with two CN^- and an electron-donor L ligand (such as CH_3S^-) is sufficient to modify the structure of the bimetallic cluster

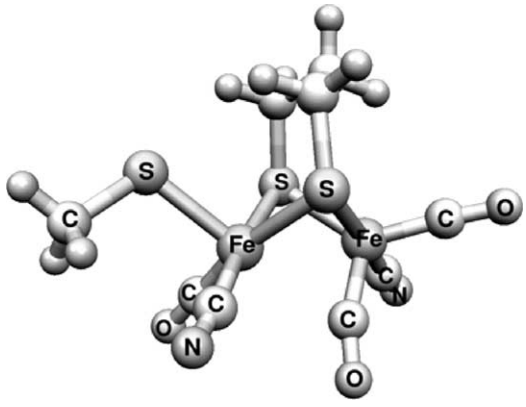

Fig. 10. DFT-optimized structure of the Fe(I)Fe(I) model complex $[(\mu\text{-PDT})Fe_2(CO)_3(CN)_2(CH_3S)]^{3-}$.

from a pseudo-symmetrical edge-bridged square pyramid to a μ-CO species characterized by a vacant coordination site on Fe_d. The latter observation is crucial because it suggests that the protein environment does not affect significantly the structural properties of the bimetallic cofactor. The extension of the study to Fe(II)Fe(I) models [83], which correspond to the paramagnetic form of the $[2Fe]_H$ cluster, confirmed previous evidences [78] indicating that these species can exist in two almost iso-energetic isomers, characterized either by the presence or absence of a CO group bridging the two metal centres. In particular, the μ-CO forms were found to be always slightly more stable, in agreement with the observation of a bridging CO group in the partially oxidized form of the enzyme [9]. Notably, the substitution of soft L ligands with relatively hard species such as CH_3S^- systematically decreases the energy gap. Moreover, it was noted that when L is a relatively hard ligand, the interconversion of μ-CO to CO-unbridged forms implies only the concerted movement of the two CO ligands coordinated to Fe_d, whereas the position of the CN^- group, which in the enzyme is strongly anchored to the protein backbone via hydrogen bonding interactions, does not change significantly in the two isomers (Fig. 8). These observations suggest that CO-unbridged Fe(II)Fe(I) forms might be transiently formed in the catalytic cycle of the enzyme. Moreover, the marked influence of the electronic properties of L on the chemistry of the bimetallic cluster suggests also that the oxidation state of the proximal $[Fe_4S_4]$ cluster could affect the structural and electronic properties of the $[2Fe]_H$ cluster, possibly modulating the relative stability of μ-CO and CO-unbridged forms.

The analysis of structural and electronic properties of Fe(I)Fe(I) models related to the fully reduced form of the $[2Fe]_H$ cluster is relevant to unravel key factors affecting binding of H^+ to the metal cofactor. Darensbourg and coworkers [80] showed that, as a result of rotation of the $Fe(CO)_3$ group, the highest occupied molecular orbital (HOMO) of the cluster changes significantly, resulting in a partial disruption of the Fe–Fe bond density and development of a charge dipole along the Fe–Fe axis. In particular, the iron centre bound to the rotated CO groups, which correspond to Fe_d in the $[2Fe]_H$ subcluster, becomes more electrophilic. Note that this latter observation may suggest that Fe_d is not the binding site of H^+. On the other hand, in CO-unbridged forms both metal ions have a pronounced nucleophilic character. In fact, the experimental investigation of cleverly designed Fe(I)Fe(I) organometallic complexes showed that oxidative addition of H^+ leads to species in which the hydride bridges the two iron centres [84,85].

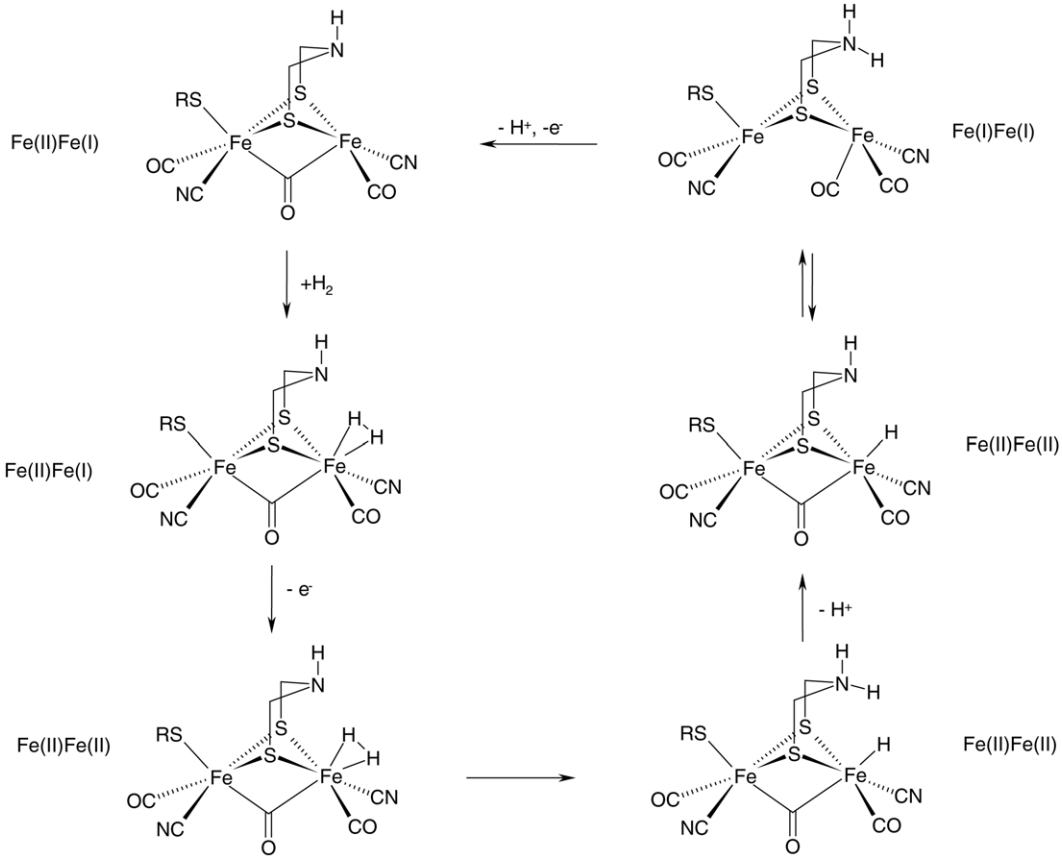

Fig. 11. Catalytic cycle of [Fe] hydrogenases proposed by Cao and Hall [74], and Liu and Hu [76] on the ground of DFT investigations.

2.3.3. Binding and activation of dihydrogen on models of the $[2Fe]_H$ cluster

Possible binding modes of H_2 to the bimetallic cluster, as well as pathways for H_2 heterolytic cleavage, have been investigated by several groups. Cao and Hall used DFT to study H_2 heterolytic cleavage taking place on Fe_d [74], which has been suggested to be the site of H_2 binding and activation on the basis of X-ray data [9]. It turned out that cleavage of H_2 on the Fe(II)Fe(II) complex $[(H_2)(CO)_2(CN)Fe(\mu\text{-PDT})Fe(CO)(CN)(SMe)]^-$, accompanied by protonation of a μ_2-S ligand, is characterized by an activation energy higher than 17 kcal mol^{-1}. In addition, the product lies 15.3 kcal mol^{-1} above the starting H_2 complex. On the other hand, the proton transfer to one of the CN^- ligands is characterized by a very large barrier (37.8 kcal mol^{-1}) even if the product is slightly more stable (-0.3 kcal mol^{-1}) than the dihydrogen complex. Therefore, it was concluded that the cleavage of H_2 on the distal Fe_d atom of the Fe(II)Fe(II) complex $[(H_2)(CO)_2(CN)Fe(\mu\text{-PDT})Fe(CO)(CN)(SMe)]^-$ is kinetically or thermodynamically unfavourable. However, if the PDT group is substituted by DTMA, the heterolytic cleavage of H_2 mediated by the N atom of the chelating ligand was shown to be kinetically favorable ($\Delta E^{\ddagger} = 6.53$ kcal mol^{-1}) [86]. Furthermore, the product of the reaction is only 2.6 kcal mol^{-1} above the reactants. On the ground of DFT results and assuming that a DTMA moiety bridges the iron atoms, Hall and coworkers [74,86] proposed a catalytic cycle (Fig. 11) where H_2 initially binds to the vacant coordination site of a μ-CO Fe(II)Fe(I) species. Binding of H_2 triggers one-electron oxidation of the $[2Fe]_H$ cluster, leading to a Fe(II)Fe(II) species where the heterolytic cleavage of H_2 can take place. This step produces a formal Fe(II)Fe(II) species characterized by a protonated DTMA group and a terminal hydride coordinated to Fe_d. Then, this intermediate can release H^+, probably from the protonated amino group of DTMA, which can then act again as a base and bind the H^+ released by Fe_d. This latter proton transfer is accompanied by formal two-electron reduction of the bimetallic cluster, leading to a CO semi-bridged Fe(I)Fe(I) species correspondent to the fully reduced form of the $[2Fe]_H$ cluster. One-electron oxidation of the cluster and proton release from DTMA close the catalytic cycle. Similar conclusions were reached by Liu and Hu [76].

Even if the mechanism proposed by Hall and coworkers [74,86] and Liu and Hu [76] fits well with available experimental and theoretical results, the evidences for the presence of DTMA in the enzyme active site are only indirect and other H_2 activation pathways might be operative in the enzyme. The investigation of alternative routes to H_2 heterolytic cleavage can be relevant also to better understand the chemistry of synthetic coordination compounds and possibly drive the design of new catalysts. Prompted by

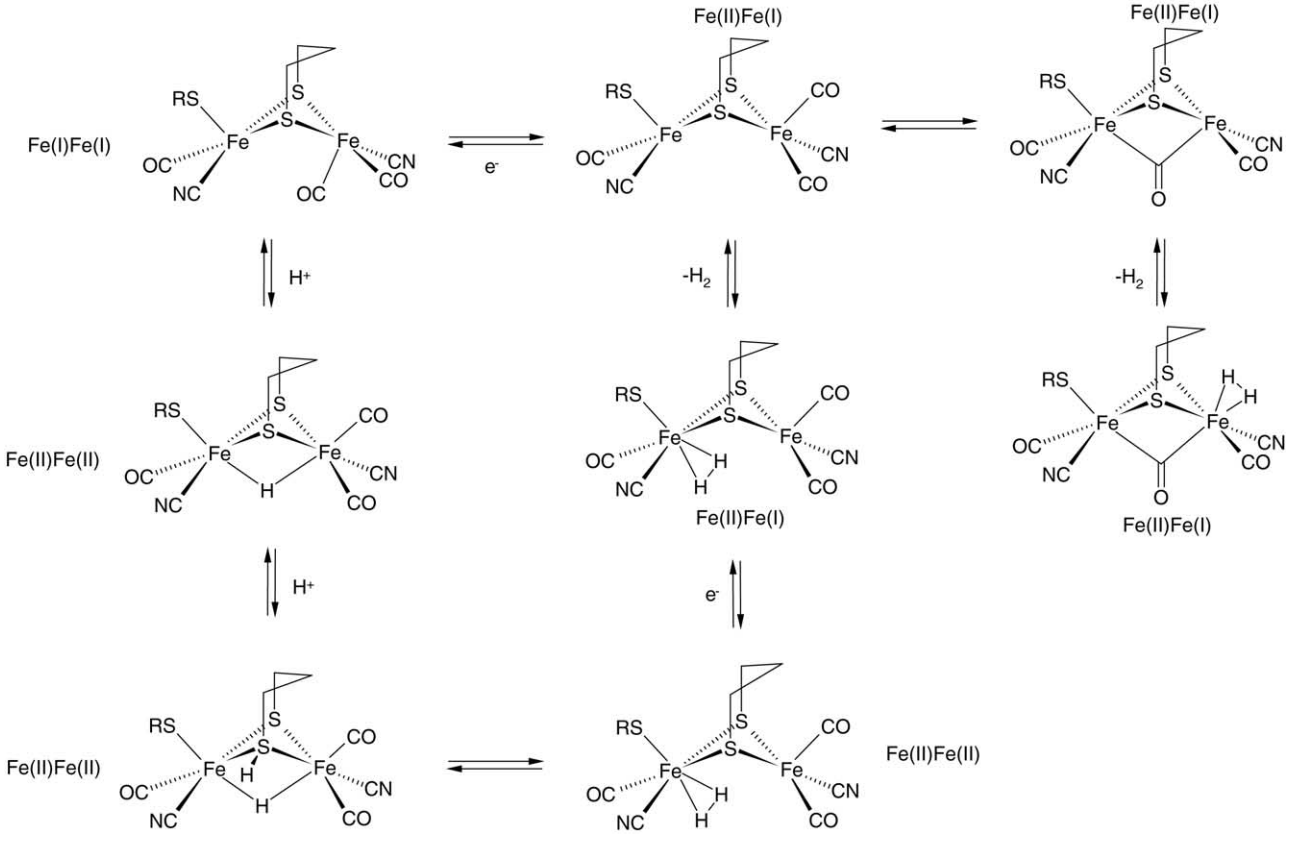

Fig. 12. Plausible catalytic cycle for [Fe] hydrogenases, not involving a DTMA ligand, proposed by Bruschi et al. [77,78,83] on the ground of DFT investigations.

theoretical evidences indicating that the interconversion between $[2Fe]_H$ models characterized by bridged and terminal CO is facile [77], Bruschi et al. have investigated H_2 binding and activation on the models system $[(CO)_2(CN)Fe(\mu\text{-}PDT)Fe(CO)(CN)(CH_3S)]^-$ leading to μ-H intermediate species [78]. It turned out that H_2 can bind to both iron atoms and that the relative stabilities of the H_2 adducts are very similar. In addition, when H_2 is bound to Fe_p, it can undergo heterolytic cleavage resulting in transfer of H^+ to a μ_2-S atom of PDT and simultaneous coordination of H^- to both metal centres (Fig. 7b and c). The computed energy barrier is as low as 5.3 kcal mol^{-1} and the products were computed to be only 2.4 kcal mol^{-1} less stable than the reactants. In fact, the possible formation in the catalytic cycle of intermediate μ-H species similar to those first characterized by Poliblanc and coworkers [87], was predicted also by Cao and Hall [74]. Moreover, the experimental characterization of synthetic models have shown that ligands with better donor ability than CO promote the binuclear oxidative addition of H^+ to yield [Fe(II)(μ-H)Fe(II)] species [84]. In light of the above considerations and DFT results, a plausible catalytic cycle that does not imply the presence of the DTMA ligand has been proposed [78] (Fig. 12). The Fe(II)Fe(I) species characterized by a vacant coordination position on Fe_d, as observed in the X-ray structure of the enzyme, can bind H_2 but, when the chelating ligand is PDT, is not capable to promote H_2 heterolytic cleavage, even assuming previous one-electron oxidation of the cluster [74]. However, the coordinatively unsaturated μ-CO Fe(II)Fe(I) species is predicted to be in equilibrium with the CO-unbridged Fe(II)Fe(I) isomer that can bind H_2 to Fe_p. H_2 coordination may trigger one-electron oxidation leading to a Fe(II)Fe(II) species where H_2 heterolytic cleavage can take place according to a pathway which is both kinetically and thermodinamically favourable. This key reaction step leads to a Fe(II)Fe(II) species characterized by a hydride bridging the two iron ions. Extraction of a proton results in a Fe(I)Fe(I) CO-semibridged form correspondent to the fully reduced $[2Fe]_H$ cluster characterized by X-ray diffraction [9,18]. Subsequent mono-electron oxidation restores the initial Fe(II)Fe(I) species and closes the catalytic cycle. Zhou et al. have recently reached very similar conclusions [88], showing also that a μ-H Fe(II)Fe(II) intermediate could not easily accept an electron because all the low-lying 3d bonding orbitals of the iron ions

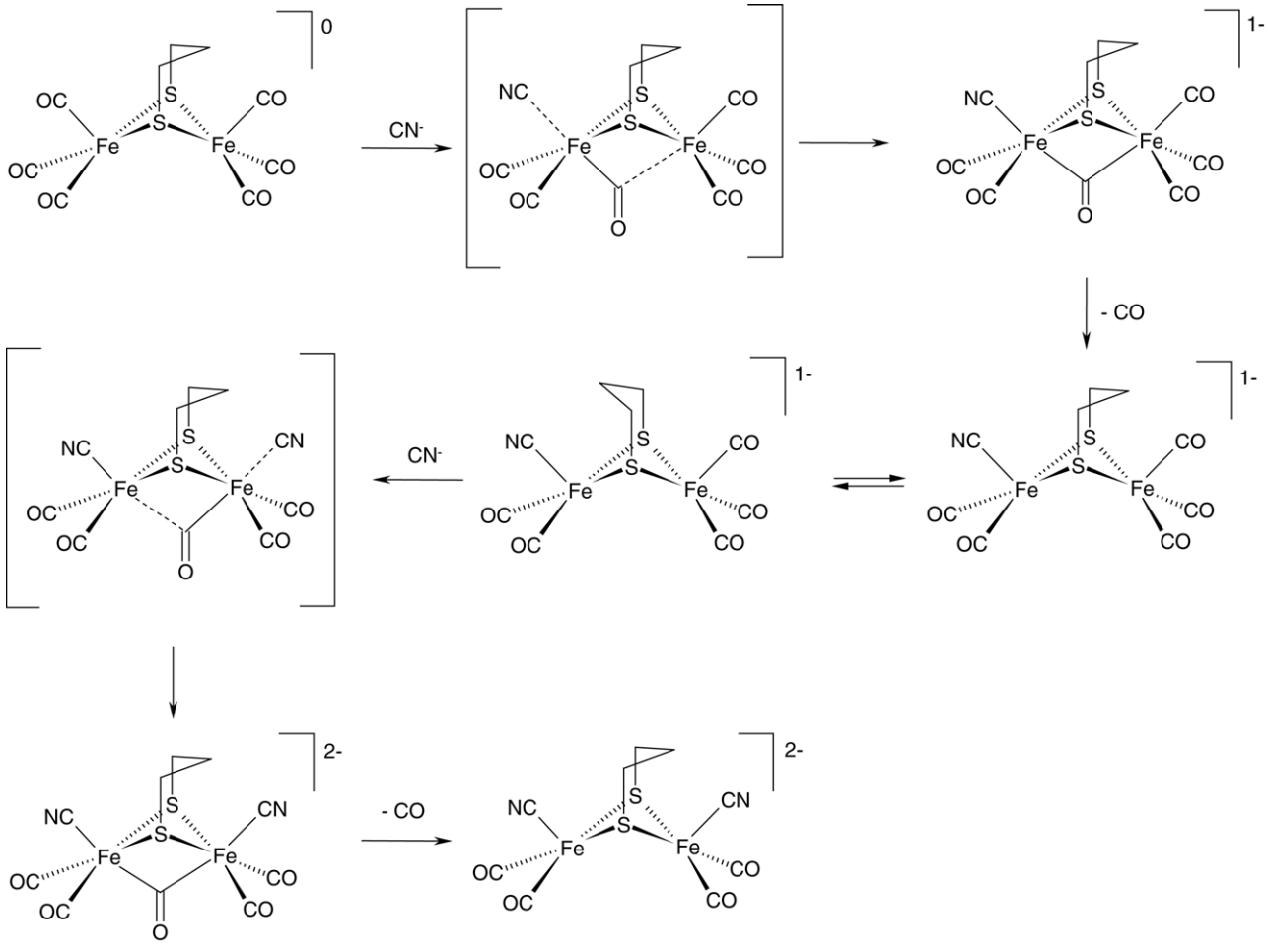

Fig. 13. DFT dissection of the reaction path for the cyanation of $[Fe_2(\mu\text{-}PDT)(CO)_6]$, as obtained by Darensbourg and coworkers [80].

are fully occupied and the LUMO is characterized by a very high energy. Consequently, the μ-H Fe(II)Fe(II) species is predicted to be nucleophilic and able to bind another proton.

2.4. DFT investigations of synthetic models related to the $[2Fe]_H$ cluster

The similarity between the $[2Fe]_H$ cluster and organometallic Fe(I)Fe(I) complexes characterized by the general structure $[Fe_2(\mu\text{-}SR)_2(CO)_6]$ stimulated the exploration of synthetic routes leading to structural and functional models of the [Fe] hydrogenase active site [26–28,89]. Such investigations were also relevant to shed light on possible pathways leading to the biosynthesis of the cofactor, as well as to understand the evolutionary process that led to biologically compatible catalysts [90]. However, some relevant issues related to the reactivity of this class of compounds could not be easily addressed experimentally, mainly due to the difficulties arising in the characterization of short-lived intermediates and transition states. As an example, Rauchfuss and coworkers shown evidences for the formation of short-lived μ-CO intermediate species [91], which are difficult to characterize experimentally but are very relevant in light of the presence of a μ-CO group in the enzymatic $[2Fe]_H$ cluster. In this context, DFT has been recently used to nicely complement the experimental investigation of the reactivity of bimetallic clusters related to the $[2Fe]_H$ subunit. In particular, theoretical results have provided an insight into transition states involved in substitution at di-nuclear carbonyl species, into the role of bridging CO in such substitution pathways, as well as into the role played by neighboring groups.

Darensbourg and coworkers [80] used B3LYP to study the cyanation of the complex $[Fe_2(\mu\text{-pdt})(CO)_6]$. In fact, kinetic studies established that the CN/CO substitution leading to $[Fe_2(SCH_2CH_2CH_2S)(CO)_4(CN)_2]^{2-}$ is a two-step process in which both steps follow an associative pathway [79]. Remarkably, the second cyanation step turned out to be faster than the first, an unexpected result in light of the observation that the second step implies the reaction between two anionic species. According to DFT results, in the first step of the nucleophilic attack the CN^- group approaches the least sterically hindered iron ion, and in the transition state the rotation of the $Fe(CO)_3$ unit is concurrent to the approach of CN^- to the metal centre (Fig. 13). The computed free energy of activation is 13.6 kcal mol^{-1}. In the first intermediate species formed along the cyanation pathway one CO bridges the two iron ions. The second step of the substitution reaction is preceded by the flip of the PDT linker to generate the isomer in which the remaining $Fe(CO)_3$ is unhindered. Then,

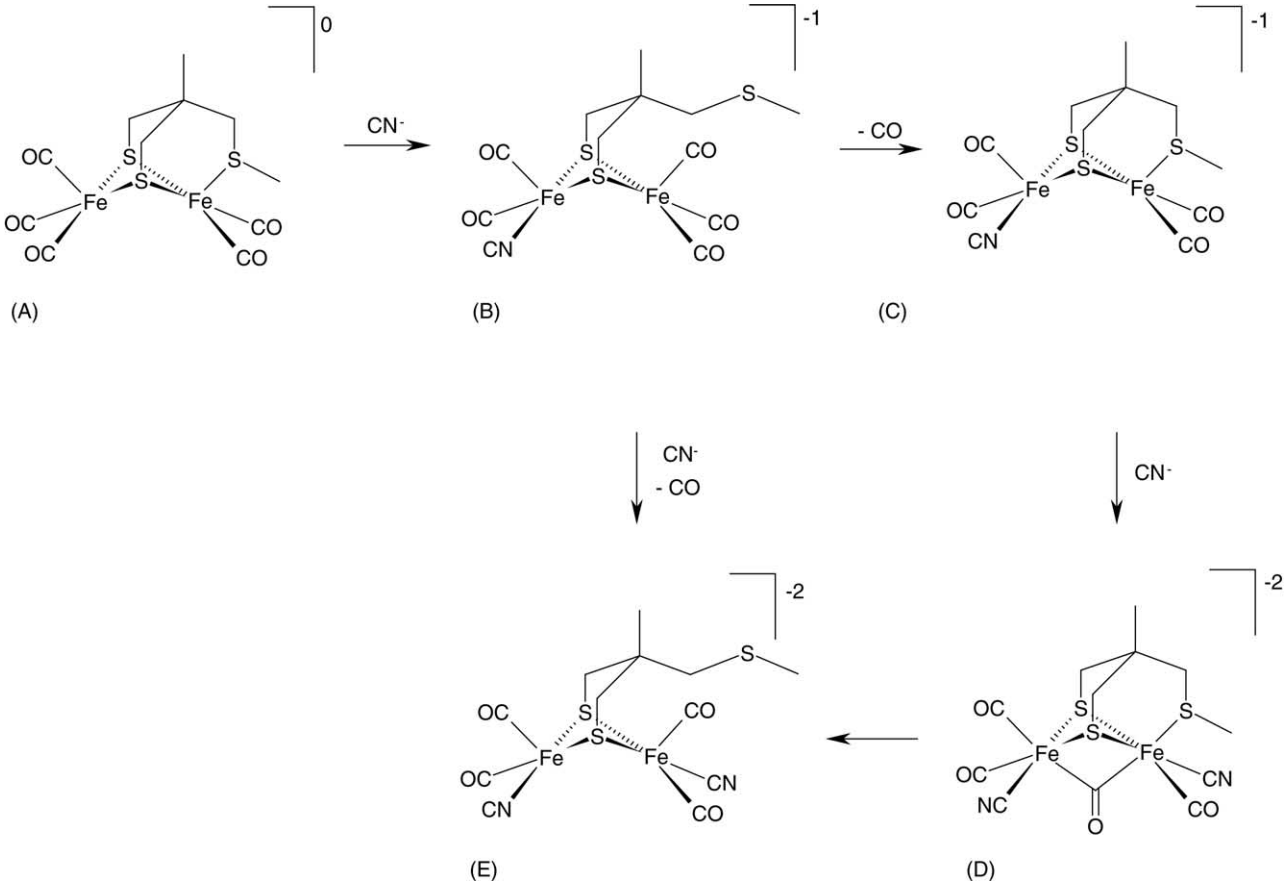

Fig. 14. Summary of the cyanation chemistry of A, as inferred by experimental investigations [92].

similarly to the first cyanation step, as CN^- approaches the iron atom, the $Fe(CO)_3$ unit rotates leading to a transition state characterized by a semibridging CO. The computed activation energy for the second step is 1.17 kcal mol^{-1} larger than for the first step. The disagreements with experimental data, which are compatible with the second cyanation being faster then the first, are due to the presence of Na^+ counterions in the computational model [80].

The synthesis and characterization of coordination compounds reproducing the $[Fe_2S_3]$ ligation observed in the $[2Fe]_H$ cluster was experimentally addressed by Pickett and coworkers [92]. According to experimental results, the initial reaction of the parent complex $[Fe_2(CO)_5(MeSCH_2C(Me)(CH_2S)_2)]$ (A) with cyanide takes place regioselectively at the Fe atom distal to the thioether ligand, leading to a monocyanide intermediate $[Fe_2(CO)_5$

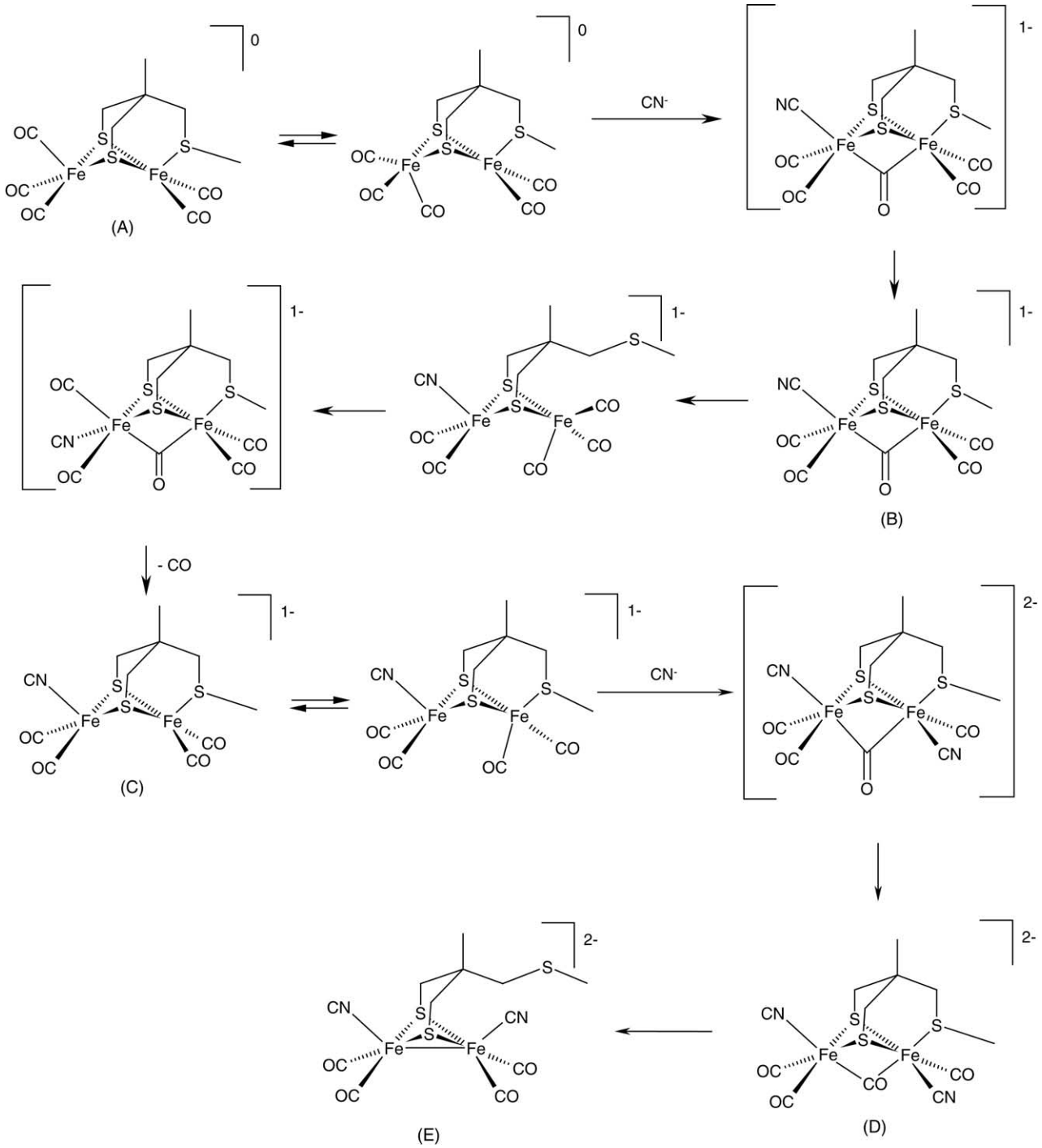

Fig. 15. Summary of the cyanation chemistry of A, as inferred by DFT calculations [46].

$(CN)(MeSCH_2C(Me)(CH_2S)_2)]$ (B) in which the thioether group is not coordinated to the iron ion (Fig. 14). B slowly loses CO to form C. The reaction of C with cyanide results in the formation of a dicyanide species which, on the basis of FT-IR spectra, has been characterized as $[Fe_2(CO)_4(\mu\text{-}CO)(MeSCH_2C(Me)(CH_2S)_2)(CN)_2]^{2-}$ (D). This species, which has the key attributes of the $[2Fe]_H$ cluster (Fe_2S_3 core and bridging CO), slowly rearranges to the thermodynamically stable product $[Fe_2(CO)_4(MeSCH_2C(Me)(CH_2S)_2)(CN)_2]^{2-}$ (E), in which the bridging carbonyl has switched to a terminally bound mode. Experimental data indicate that the initial cyanation of the Fe_2S_3-complex A takes place via an associative mechanism. However, the reaction rate for mono-cyanation of the Fe_2S_3 species A is about 10,000-fold larger than that observed for corresponding Fe_2S_2 species [26]. Other major differences are related to the substitution of CO by a second cyanide ligand. In particular, the second cyanation step taking place on the Fe_2S_3 species is kinetically hindered with respect to corresponding Fe_2S_2 complexes. In addition, spectroscopic data are consistent with the presence of a μ-CO group in D, whereas no long-lived intermediates featuring bridging CO have been characterized along the pathway to $[(\mu\text{-}pdt)Fe_2(CO)_4(CN)_2]^{2-}$. With the aim of better understanding the chemistry of Fe_2S_3 complexes and complement the kinetic and spectroscopic characterization of intermediate species along the cyanation pathway, Zampella et al. have recently reported the DFT investigation of the mechanism of cyanation of the Fe_2S_3 complex A [46]. As postulated from kinetic studies [92], the first cyanation step implies the formation of a transition state characterized by a CO group bridging the two metal ions (Fig. 15). The low energy barrier was shown to be due to the presence of the thioether group, which stabilize μ-CO species. The kinetic differences between Fe_2S_2 and Fe_2S_3 complexes in the second cyanation step were proposed to be due to deactivation of the Fe ion, caused by coordination of the thioether moiety, as well as by hindered rotation of the reacting FeL_3 group. Moreover, the correspondence of calculated and experimental infra-red data fully supported the structural assignment of the μ-CO species D [92]. Remarkably, all DFT studies aimed at clarifying the cyanation of complexes related to the $[2Fe]_H$ cluster confirm that the formation of bridging carbonyl intermediates is a key step in the synthesis of this class of compounds [80,46].

DFT calculations have been successfully used to clarify the structural and electronic properties of other synthetic models related to the metal cofactor. The properties of di-iron azadithiolate complexes, which are relevant model complexes of the $[2Fe]_H$ subunit, have been investigated by Rauchfuss and coworkers [27]. In particular, it was shown that the experimentally characterized structural properties of $[Fe_2(SCH_2NMeCH_2S)(CO)_6]$ result from a balance between the anomeric effect, which favours the axial disposition of the methyl group, and a competing steric repulsion between the axial methyl and one carbonyl ligand. Rauchfuss and coworkers have also investigated, experimentally and by DFT calculations, the regiochemistry of protonation in bimetallic carbonyl thiolates [85]. Remarkably, and differently from usual metal cyano complexes [93], it turned out that protonation at the Fe–Fe bond is competitive with protonation at CN. In addition, the site of protonation is subtly dependent on the coligands and occurs more favourably at the Fe–Fe bond for $[Fe_2(SCH_2CH_2CH_2S)(CN)(CO)_4(PMe_3)]^-$ than for $[Fe_2(SCH_2CH_2CH_2S)(CN)(CO)_4(PH_3)]^-$ or $[Fe_2(SCH_2CH_2CH_2S)(CN)(CO)_4(P(OMe)_3)]^-$ complexes.

Structures and vibrational frequencies for a series of $[Fe(CN)_x(CO)_y]$ complexes have been recently investigated at the BP86 level of theory, showing that computed Fe–CO bond distances are in very close agreement with X-ray data, whereas the Fe–CN bond lenghts are generally slightly overestimated [94]. In addition, the Fe–CO covalent bonding is characterized by a significant contribution of the π interaction, while the Fe–CN bonds have much less pronounced π character.

3. Conclusions and perspectives

Important progresses in understanding the way hydrogen is produced or oxidized by [NiFe] and [Fe] hydrogenases have been made in the last few years, due to results obtained in the fields of genetics, structural biology, spectroscopy, electrochemistry and synthetic and theoretical chemistry. However, in spite of key results obtained investigating [NiFe] and [Fe] hydrogenases, as well as related synthetic models, the available data are still incomplete and sometimes difficult to be interpreted, mainly due to the complexity of the systems and to the elusive nature of H_2 and of intermediate species formed along the $H_2 \leftrightarrows 2H^+ + 2e^-$ pathway. Consequently, some aspects of hydrogenase chemistry are still poorly understood and controversial [95]. Nevertheless, some conclusions can be drawn on the ground of recent theoretical results. DFT investigations of models of [NiFe] hydrogenases converge on the proposal that H_2 is initially bound to a Ni(II)Fe(II) species that should correspond to Ni-SI. Moreover, H_2 activation and cleavage is thought to imply the formation of μ-H species. In particular, the possibility that Ni-C corresponds to a μ-H Ni(III)Fe(II) species is now theoretically well grounded and in full agreement with spectroscopic data. Finally, results converge on the proposal that Fe(II) does not change oxidation state and remains in the low spin configuration throughout the catalytic cycle. However, other issues related to the nature of intermediate species formed in the catalytic cycle of [NiFe] hydrogenases are still controversial and require further investigations. It is unclear whether H_2 activation takes place on iron or nickel, the redox state of the Ni ion in the H_2 heterolytic cleavage step is controversial and both a cysteine residue and a water molecule have been proposed to be involved in H_2 activation. Moreover, further theoretical and experimental studies are necessary to corroborate the recent evidences for the formation of high spin species and to clarify their role in the catalytic cycle.

The theoretical investigations of models of the [Fe] hydrogenase active site has contributed to the characterization of the redox states of the $[2Fe]_H$ cluster. Both theoretical and experimental evidences converge on the proposal that Fe(I)Fe(I), Fe(II)Fe(I) and Fe(II)Fe(II) species are formed in the catalytic cycle. In addition, DFT studies suggest that H_2 activation takes place on a Fe(II)Fe(II) species. In particular, it has been shown that the heterolytic cleavage of H_2 can be mediated by a group belonging to the $[2Fe]_H$ cluster, such as the NH group of the chelating DTMA ligand or a S atom of PDT. If DTMA is the chelating ligand in the $[2Fe]_H$ cluster, H_2 cleavage can take place without the formation of a μ-H intermediate species. However, experimental and DFT results indicate that protonation of dinuclear coordination compounds related to the $[2Fe]_H$ cofactor usually takes place at the Fe–Fe bond. Also in this case, further investigations are necessary to clarify these issues. In this context, it should be noted that the presence of a DTMA ligand, which can play the role of the base in the H_2 heterolytic cleavage, is not incompatible with the formation of μ-H species, as suggested recently also by Lomoth and coworkers on the ground of the catalytic properties of synthetic models of the $[2Fe]_H$ cluster [96]. Further exploration of the factors governing the protonation site, as well as the catalytic relevance of terminal and bridged hydride species are also necessary. Finally, the role of the proximal $[Fe_4S_4]$ cluster in modulating the electronic and structural properties of the $[2Fe]_H$ cluster is still largely unexplored.

Even though [NiFe] and [Fe] hydrogenases are evolutionary uncorrelated, the metal cofactors thought to be directly involved in H_2 activation show some structural similarity (Fig. 1). In both enzymes, the catalytic cluster is dinuclear, it is bound to the protein via cysteine residues, thiolate groups bridges the two metal centres, and biologically 'unusual' CO and CN ligands are coordinated to iron ions. The common features might be an example of convergent evolution and consequently the elucidation of their role is expected to be important to design novel catalysts. However, the structural resemblance between the [NiFe] and [Fe] hydrogenase active site does not necessarily imply an identical catalytic strategy to activate H_2. Indeed, the active sites of [NiFe] and [Fe] hydrogenases can be considered similar in quite different ways (Fig. 16). Moreover, it has been noted that H_2 oxidation and proton reduction might involve separate catalytic cycles be-

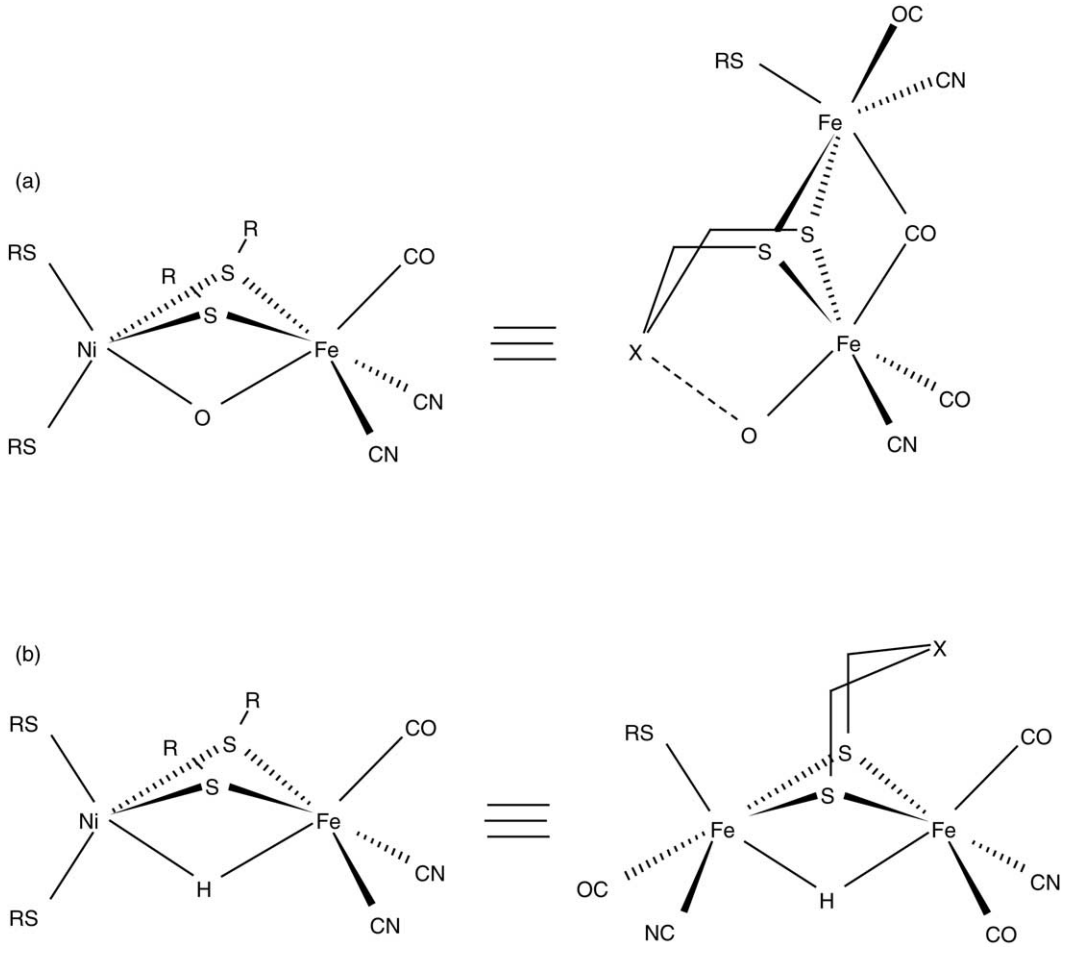

Fig. 16. Similarity between the active sites of [NiFe] and [Fe] hydroganases, as proposed by Fontecilla-Camps and coworkers [18] (a) and by the authors of this review (b).

cause these two processes are driven by respective energy sources [95]. Therefore, the theoretical comparison of the catalytic properties of models related to the active site of [NiFe] and [Fe] hydrogenases models, as well as the design and computational characterization of 'hybrid' models, could be relevant to shed light on the essential requirement for catalysis and drive experimental efforts aimed at the synthesis of new catalysts.

In conclusion, different research groups have used different computational strategies to investigate the elusive properties of the binuclear clusters found in [NiFe] and [Fe] hydrogenases. Complementary approaches have often led to similar conclusions that, most importantly, well fitted to or even predicted experimental results. In fact, recent studies have clearly showed that the symbiotic relationship between 'in silico' and 'wet' coordination chemistry can successfully lead to a better understanding of the properties of organometallic compounds related to the metallic cofactors found in [NiFe] and [Fe] hydrogenases [14,27,46,52,80]. The evolution of such interplay is anticipated to be crucial to clarify issues that are still controversial.

References

[1] S.P. Albracht, Biochim. Biophys. Acta 1188 (1994) 167;
E.G. Graf, R.K. Thauer, FEBS Lett. 136 (1981) 165;
M.W.W. Adams, Biochim. Biophys. Acta 1020 (1990) 115;
R. Cammack, Nature 397 (1999) 214;
Y. Nicolet, B.J. Lemon, J.C. Fontecilla-Camps, J.W. Peters, Trends Biochem. Sci. 25 (2000) 138;
J.W. Peters, Curr. Opin. Struct. Biol. 9 (1999) 670;
D.S. Horner, B. Heil, T. Happe, T.M. Embley, Trends Biochem. Sci. 27 (2002) 148;
Y. Nicolet, C. Cavazza, J.C. Fontecilla-Camps, J. Inorg. Biochem. 91 (2002) 1;
R. Cammack, M. Frey, R. Robson (Eds.), Hydrogen as Fuel—Learning from Nature, Taylor and Francis, London, 2001.

[2] E.J. Lyon, S. Shima, G. Buurman, S. Chowdhuri, A. Batschauer, K. Steinbach, R.K. Thauer, Eur. J. Biochem. 271 (2004) 195.

[3] A. Volbeda, M.H. Charon, C. Piras, E.C. Hatchikian, M. Frey, J.C. Fontecilla-Camps, Nature 373 (1995) 580.

[4] A. Volbeda, E. Garcin, C. Pieras, A.L. De Lacey, V.M. Fernandez, E.C. Hatchikian, M. Frey, J.C. Fontecilla-Camps, J. Am. Chem. Soc. 118 (1996) 12989.

[5] E. Garcin, X. Vernede, E. C: Hatchikian, A. Volbeda, M. Frey, J.C. Fontecilla-Camps, Structure 7 (1999) 557.

[6] Y. Higuchi, T. Yagi, N. Yasuoka, Structure 5 (1997) 1671.

[7] Y. Higuchi, H. Ogata, K. Miki, N. Yasuoka, T. Yagi, Structure 7 (1999) 549.

[8] H. Ogata, Y. Mizoguchi, N. Mizuno, K. Miki, S. Adachi, N. Yasuoka, T. Yagi, O. Yamauchi, S. Hirota, Y. Higuchi, J. Am. Chem. Soc. 124 (2002) 11628.

[9] Y. Nicolet, C. Piras, P. Legrand, E.C. Hatchikian, J.C. Fontecilla-Camps, Structure 7 (1999) 13;
J.W. Peters, W.N. Lanzilotta, B.J. Lemon, L.C. Seefeldt, Science 282 (1998) 1853.

[10] K.A. Bagley, E.C. Duin, W. Roseboom, S.P. Albracht, W.H. Woodruff, Biochemistry 34 (1995) 5527;
R.P. Happe, W. Roseboom, A.J. Pierik, S.P. Albracht, K.A. Bagley, Nature 385 (1997) 126.

[11] V.M. Fernandez, E.C. Hatchikian, R. Cammack, Biochim. Biophys. Acta 832 (1985) 69.

[12] M. Teixeira, I. Mora, G. Fauque, M. Czechowski, Y. Berlier, P. A: Lespinat, J. LeGall, A.V. Xavier, J.J.G. Moura, Biochimie 68 (1986) 75.

[13] L.M. Roberts, P.A. Lindahl, Biochemistry 33 (1994) 14339;
A.L. de Lacey, E.C. Hatchikian, A. Volbeda, M. Frey, J.C. Fontecilla-Camps, V.M. Fernandez, J. Am. Chem. Soc. 119 (1997) 7181.

[14] A.L. de Lacey, C. Stadler, V.M. Fernandez, E.C. Hatchikian, H.-J. Fan, S. Li, M.B. Hall, J. Biol. Inorg. Chem. 7 (2002) 318–326.

[15] C.V. Popescu, E. Munck, J. Am. Chem. Soc. 121 (1999) 7877.

[16] A. de Lacey, C. Stadler, C. Cavazza, E.C. Hatchikian, V.M. Fernandez, J. Am. Chem. Soc. 122 (2000) 11232;
A.S. Pereira, P. Tavares, I. Moura, J.J.G. Moura, B.H. Huynh, J. Am. Chem. Soc. 123 (2001) 2771;
B. Bennet, B.J. Lemon, J.W. Peters, Biochemistry 39 (2000) 7455.

[17] B.J. Lemon, J.W. Peters, Biochemistry 38 (1999) 12969.

[18] Y. Nicolet, A.L. de Lacey, X. Vernede, V.M. Fernandez, E. C: Hatchikian, J.C. Fontecilla-Camps, J. Am. Chem. Soc. 123 (2001) 1596.

[19] D.J. Evans, C.J. Pickett, Chem. Soc. Rev. 35 (2003) 268;
T.B. Rauchfuss, Inorg. Chem. 43 (2004) 14.

[20] M.Y. Darensbourg, E.J. Lyon, J.J. Smee, Coord. Chem. Rev. 206–207 (2000) 533.

[21] F. Osterloh, W. Saak, D. Hasse, S. Pohl, Chem. Commun. (1997) 979.

[22] S.C. Davies, D.J. Evans, D.L. Hughes, S. Longhurst, J.R. Sanders, Chem. Commun. (1999) 1935;
M.C. Smith, J.E. Barclay, S.P. Cramer, S.C. Davies, W.-W. Gu, D.L. Hughes, S. Longhurst, D.J. Evans, J. Chem. Soc., Dalton Trans. (2002) 2641.

[23] A.C. Marr, D.J.E. Spencer, M. Schroder, Coord. Chem. Rev. 206–207 (2000) 1055.

[24] D. Sellman, F. Geipel, F. Lauderbach, F.W. Heinemann, Angew. Chem. Int. Ed. 41 (2002) 632.

[25] H. Reihlen, A. Gruhl, G. Hessling, Liebigs Ann. Chem. 472 (1929) 268;
D. Seyferth, G.B. Womack, C.M. Archer, J.C. Dewan, Organometallics 8 (1989) 430.

[26] E.J. Lyon, I.P. Georgakaki, J.H. Reibenspies, M.Y. Darensbourg, Angew. Chem., Int. Ed. 38 (1999) 3178;
A. Le Cloirec, S.P. Best, S. Borg, S.C. Davies, D.J. Evans, D.L. Hughes, C.J. Pickett, Chem. Commun. (1999) 2285;
M. Schmidt, S.M. Contakes, T.B. Rauchfuss, J. Am. Chem. Soc. 121 (1999) 9736.

[27] J.D. Lawrence, H. Li, T.B. Rauchfuss, M. Benard, M.-M. Rohmer, Angew. Chem. Int. Ed. 40 (2001) 1768.

[28] M. Razavet, S.C. Davies, D.L. Hughes, C.J. Pickett, Chem. Commun. (2001) 847.

[29] L-C. Song, Z.-Y. Yang, H.-Z. Bian, Q.-M. Hu, Organometallics 23 (2004) 3082–3084.

[30] S. Niu, M.B. Hall, Chem. Rev. 100 (2000) 353;
P.E.M. Siegbahn, M.R.A. Blomberg, Chem. Rev. 100 (2000) 421;
T. Lovell, F. Himo, W.-G. Han, L. Noodleman, Coord. Chem. Rev. 238–239 (2003) 211;
R.A. Friesner, M.-H. Baik, B.F. Gherman, V. Guallar, M. Wirstam, R.B. Murphy, S.J. Lippard, Coord. Chem. Rev. 238–239 (2003) 267.

[31] P.E.M. Siegbahn, M.R.A. Blomberg, M. Wirstam Pavlov, R.H. Crabtree, J. Biol. Inorg. Chem. 6 (2001) 460;
H.-J. Fan, M.B. Hall, J. Biol. Inorg. Chem. 6 (2001) 467;
M. Stein, W. Lubitz, Curr. Opin. Chem. Biol. 6 (2002) 243.

[32] M. Pavlov, P.E.M. Siegbahn, M.R.A. Blomberg, R.H. Crabtree, J. Am. Chem. Soc. 129 (1998) 548.
[33] R.G. Parr, W. Yang, Density Functional Theory of Atoms and Molecules, Oxford University Press, New York, 1989.
[34] L. Turker, I. Eroglu, M. Yucel, U. Gunduz, J. Mol. Struct. Theochem. 672 (2004) 169;
L. Turker, J. Mol. Struct. Theochem. 664–665 (2003) 175.
[35] W. Koch, M.C. Holthausen, A Chemist's Guide to Density Functional Theory, second ed. Wiley Ed, 2002.
[36] P. Hohenberg, W. Kohn, Phys. Rev. 136 (1964) B864.
[37] I. Levine, Quantum Chemistry, fifth ed., Prentice Hall, 1999.
[38] The term "spin contamination" refers to the computed <S2> value that in the unrestricted formalism is always larger than the expectation value of a pure spin state S(S+1). This is due to the non orthogonality of the α and β spin orbitals that causes, differently from the restricted formalism, the wavefunction not to be an eigenfuction of the <S2> operator. It should be mentioned that the physical meaning of the "spin contamination" in the DFT calculations is still a matter of debate..
[39] K. Eichkorn, O. Treutler, H. Ohm, M. Haser, R. Ahlrichs, Chem. Phys. Lett. 240 (1995) 283;
K. Eichkorn, F. Weigend, O. Treutler, R. Ahlrichs, Theor. Chem. Acc. 97 (1997) 119.
[40] A.D. Becke, J. Chem. Phys. 96 (1992) 2155;
A.D. Becke, J. Chem. Phys. 98 (1993) 5648;
P.J. Stevens, F.J. Devlin, C.F. Chablowski, M.J. Frisch, J. Phys. Chem. 98 (1994) 11623;
C. Lee, W. Yang, R.G. Parr, Phys. Rev. B 37 (1988) 785.
[41] A.D. Becke, Phys. Rev. A 38 (1988) 3098;
J.P. Perdew, Phys. Rev. B 33 (1986) 8822.
[42] V. Jonas, W. Thiel, J. Chem. Phys. 96 (1995) 8474.
[43] C.J. Cramer, Essentials of Computational Chemistry—Theories and Models, Wiley Ed, 2002.
[44] A.P. Scott, L. Radom, J. Phys. Chem. 100 (1996) 16502.
[45] M. Bruschi, L. De Gioia, G. Zampella, M. Reiher, P. Fantucci, M. Stein, J. Biol. Inorg. Chem. 9 (2004) 873.
[46] G. Zampella, M. Bruschi, P. Fantucci, M. Razavet, C.J. Pickett, L. De Gioia, Chem. Eur. J. 11 (2005) 509.
[47] J. Neugebauer, M. Reiher, C. Kind, B.A. Hess, J. Comput. Chem. 23 (2002) 895;
J. Neugebauer, B.A. Hess, J. Chem. Phys. 118 (2003) 7215.
[48] F. Neese, Curr. Opin. Chem. Biol. 7 (2003) 125.
[49] E. van Lenthe, E.J. Baerends, J.G. Snijders, J. Chem. Phys. 99 (1993) 4597;
A.J. Sadlej, J.G. Snijders, E. van Lenthe, E.J. Baerends, J. Chem. Phys. 102 (1995) 1758.
[50] S.H. Vosko, L. Wilk, M. Nusair, Can. J. Phys. 58 (1980) 1200.
[51] M. Stein, W. Lubitz, J. Inorg. Biochem. 98 (2004) 862.
[52] M. Stein, E. van Lenthe, E.J. Baerends, W. Lubitz, J. Am. Chem. Soc. 123 (2001) 5839;
M. Stein, W. Lubitz, Phys. Chem. Chem. Phys. 3 (2001) 5115;
M. Stein, W. Lubitz, Phys. Chem. Chem. Phys. 3 (2001) 2668.
[53] C. Stadler, A.L. de Lacey, B. Hernandez, V.M. Fernandez, J.C. Conesa, Inorg. Chem. 41 (2002) 4417;
C. Stadler, A.L. de Lacey, Y. Montet, A. Volbeda, J.C. Fontecilla-Camps, J.C. Conesa, V.M. Fernandez, Inorg. Chem. 41 (2002) 4424.
[54] S. Foerster, M. Stein, M. Brecht, H. Ogata, Y. Higuchi, W. Lubitz, J. Am. Chem. Soc. 125 (2003) 83.
[55] P. Amara, A. Volbeda, J.C. Fontecilla-Camps, M.J. Field, J. Am. Chem. Soc. 121 (1999) 4468.
[56] L. De Gioia, P. Fantucci, B. Guigliarelli, P. Bertrand, Inorg. Chem. 38 (1999);
L. De Gioia, P. Fantucci, B. Guigliarelli, P. Bertrand, Int. J. Quantum Chem. 73 (1999) 187.
[57] F. Dole, A. Fournel, V. Magro, E. C: Hatchikian, P. Bertrand, B. Guigliarelli, Biochemistry 36 (1997) 7847.
[58] S. Niu, L.M. Thomson, M.B. Hall, J. Am. Chem. Soc. 121 (1999) 4000.
[59] C.P. Wang, R. Franco, J.J.G. Moura, I. Moura, E.P. Day, J. Biol. Chem. 267 (1992) 7378.
[60] M. Stein, W. Lubitz, Phys. Chem. Chem. Phys. 3 (2001) 2668.
[61] H. Wang, C.Y. Ralston, D.S. Patil, R.M. Jones, W. Gu, M. Verhagen, M. Adams, P. Ge, C. Riordan, C.A. Marganian, P. Mascharak, J. Kovacs, C.G. Miller, T.J. Collins, S. Brooker, P.D. Croucher, K. Wang, E.I. Stiefel, S.P. Cramer, J. Am. Chem. Soc. 122 (2000) 10544;
W. Gu, L. Jacquamet, D.S. Patil, H.-X. Wang, D.J. Evans, M.C. Smith, M. Millar, S. Koch, D.M. Eichhorn, M. Latimer, S.P. Cramer, J. Inorg. Biochem. 93 (2003) 41.
[62] H.-J. Fan, M.B. Hall, J. Am. Chem. Soc. 124 (2002) 394.
[63] W. Koch, M.C. Halthausen, A Chemist's Guide to Density Functional Theory, second ed., Wiley, 2002.
[64] T.R. Cundari (Ed.), Computational Organometallic Chemistry, Marcel Dekker, New York, 2001.
[65] M. Reiher, O. Salomon, D. Sellmann, B.A. Hess, Chem. Eur. J. 7 (2001) 5195.
[66] L. Cavallo, H. Jacobsen, J. Phys. Chem. A 107 (2003) 5466;
H. Paulsen, L. Duelund, H. Winkler, H. Toftlund, A.X. Trautwein, Inorg. Chem. 40 (2001) 2201;
R. Poli, J.N. Harvey, Chem. Soc. Rev. 32 (2003) 1.
[67] I.V. Khavrutskii, D.G. Musaev, K. Morokuma, Inorg. Chem. 42 (2003) 2606.
[68] J.N. Harvey, M. Aschi, Faraday Discuss. (2003) 129.
[69] M. Reiher, O. Salomon, B.A. Hess, Theor. Chem. Acc. 107 (2001) 48.
[70] M. Reiher, Inorg. Chem. 41 (2002) 6928;
O. Salomon, M. Reiher, B.A. Hess, J. Chem. Phys. 117 (2002) 4729.
[71] S. Niu, M.B. Hall, Inorg. Chem. 40 (2001) 6201.
[72] Z. Chen, B.J. Lemon, S. Huang, D.J. Swartz, J.W. Peters, K.A. Bagley, Biochemistry 41 (2002) 2036.
[73] I. Dance, Chem. Commun. (1999) 1655.
[74] Z. Cao, M.B. Hall, J. Am. Chem. Soc. 123 (2001) 3734.
[75] A.J. Pierik, M. Hulstein, W.R. Hagen, S.P.J. Albracht, Eur. J. Biochem. 258 (1998) 572.
[76] Z.-P. Liu, P. Hu, J. Am. Chem. Soc. 124 (2002) 5175.
[77] M. Bruschi, P. Fantucci, L. De Gioia, Inorg. Chem. 41 (2002) 1421.
[78] M. Bruschi, P. Fantucci, L. De Gioia, Inorg. Chem. 42 (2003) 4773.
[79] E.J. Lyon, I.P. Georgakaki, J.H. Reibenspies, M.Y. Darensbourg, J. Am. Chem. Soc. 123 (2001) 3268.
[80] I.P. Georgakaki, L.M. Thomson, E.J. Lyon, M.B. Hall, M.Y. Darensbourg, Coord. Chem. Rev. 238–239 (2003) 255.
[81] B.L. Vallee, R.J. Williams, Proc. Natl. Acad. Sci. U.S.A. 59 (1968) 498.
[82] M.Y. Darensbourg, E.J. Lyon, X. Zhao, I.P. Georgakaki, Proc. Natl. Acad. Sci. U.S.A. 100 (2003) 3683.
[83] M. Bruschi, P. Fantucci, L. De Gioia, Inorg. Chem. 43 (2004) 3733.
[84] X. Zhao, I.P. Georgakaki, M.L. Miller, R. Mejia-Rodriguez, C.-Y. Chiang, M.Y. Darensbourg, Inorg. Chem. 41 (2002) 3917.
[85] F. Gloaguen, J.D. Lawrence, T.B. Rauchfuss, M. Benard, M.M. Rohmer, Inorg. Chem. 41 (2002) 6573.
[86] H.-J. Fan, M.B. Hall, J. Am. Chem. Soc. 123 (2001) 3828.
[87] K. Fauvel, R. Mathieu, R. Poliblanc, Inorg. Chem. 15 (1976) 976.
[88] T. Zhou, Y. Mo, A. Liu, Z. Zhou, K.R. Tsai, Inorg. Chem. 43 (2004) 923.
[89] H. Li, T.B. Rauchfuss, J. Am. Chem. Soc. 124 (2002) 726.
[90] G. Wachtershauser, Prog. Biophys. Mol. Biol. 58 (1992) 85.
[91] F. Gloaguen, J.D. Lawrence, M. Schmidt, S.R. Wilson, T.B. Rauchfuss, J. Am. Chem. Soc. 123 (2001) 12518.

[92] M. Razavet, S.J. Borg, S.J. George, S.P. Best, S.A. Fairhurst, C.J. Pickett, Chem. Commun. (2002) 700;
S.J. George, Z. Cui, M. Razavet, C.J. Pickett, Chem. Eur. J. 8 (2002) 4037;
M. Razavet, S. C: Davies, D.L. Hughes, J. E: Barclay, D.J. Evans, S.A. Fairhurst, X. Liu, C.J. Pickett, J. Chem. Soc., Dalton Trans. 4 (2003) 586.
[93] C. Bianchini, F. Laschi, M.F. Ottaviani, M. Peruzzini, P. Zanello, F. Zenobini, Organometallics 8 (1989) 893;
C. Nataro, J. Chen, R.J. Angelici, Inorg. Chem. 37 (1998) 1868.
[94] C. Loschen, G. Frenking, Inorg. Chem. 43 (2004) 778.
[95] F.A. Armstrong, Curr. Opin. Chem. Biol. 8 (2004) 133.
[96] S. Ott, M. Kritikos, B. Akermark, L. Sun, R. Lomoth, Angew, Chem. Int. Ed. 43 (2004) 1006–1009.